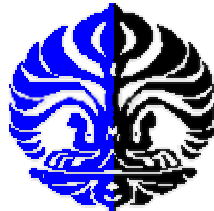


**VALIDATING THE SWEETNESS ATTRIBUTE  
AND AVO ANALYSIS IN DEFINING FLUID  
CONTACT IN BATURAJA FORMATION AT  
CANTIK FIELD, SOUTH SUMATRA BASIN**

**Thesis**



**By  
AURORA JUNIARTI  
0706171806**

**PHYSICS GRADUATE PROGRAM  
FACULTY OF MATHEMATIC AND NATURAL SCIENCE  
UNIVERSITY OF INDONESIA  
Jakarta  
2009**

## ABSTRACT

Cantik is an oil-producing field located in South Sumatra Extension Block, a Medco E&P operation area. Cantik has 10 oil producer wells. Oil in-place volumetric calculations predict approximately 4.2 MMBO, while the proven reserve is about 1.3 MMBO. From the two last drillings founded that the reservoir was tight and difficult to develop. From that point make bigger challenges to develop Cantik field.

Conventional attribute and interpretation methods provide limited access for delineating a highly heterogeneous reservoir distribution. Due to the problems of heterogeneous limestone and complex stratigraphic trap interpretation, it is difficult to develop and manage Cantik field. We need new approach to solving Cantik field problem, new approach method that can help to define reservoir distribution is defining fluid contact from various attributes.

Sweetness attribute was used to define carbonate-shale ratio, but in some case, we also can find the relationship between sweetness attribute and relative fluid content. And from AVO Analysis analysis, can be detect fluid contact distribution base on well and seismic data. Hopefully with validation of various attribute can be delineated this complex geological feature.

The validating of sweetnees attribute and AVO analysis reveals the distribution and orientation of the reservoir targets, which are consistent with well data. This method helped us to propose not only successful exploration wells but also gave us an idea about the extent of the pool. Because of this study, the risks of proposing development wells can significantly reduced.

## ABSTRAK

Cantik adalah lapangan yang memproduksi minyak yang berlokasi di Blok South Sumatra Extension, yang merupakan daerah operasi dari Medco E&P. Lapangan Cantik telah memproduksi minyak dari 10 sumur. Prediksi perhitungan dari volume oil in-place sekitar 4.2 MMBO, sampai saat ini cadangan yang telah dihasilkan sekitar 1.3 MMBO. Dari 2 sumur yang terakhir ditemukan bahwa reservoir tight dan sulit untuk diprosuksi. Hal tersebut membuat tantangan yang lebih besar lagi untuk mengembangkan lapangan ini..

Metoda atribut dan interpretasi konvensional mempunyai keterbatasan akses untuk mendelineasi distribusi reservoir dengan tingkat heterogenitas tinggi. Berdasarkan permasalahan heterogenitas dan interpretasi dari perangkat stratigrafi yang kompleks dari batugamping, menyebabkan sulitnya untuk mengembangkan dan mengelola lapangan Cantik. Kita membutuhkan suatu pendekatan yang baru untuk memecahkan masalah tersebut, pendekatan terbaru yang memungkinkan penentuan distribusi dari reservoir adalah dengan menentukan batas dari kontak fluida.

Atribut 'sweetness' menunjukkan rasio dari karbonat-serpik, namun pada kasus ini ditemukan juga korelasi atribut sweetness dengan keterdapatan fluida. Dari analisa AVO diharapkan dapat mendeteksi distribusi kontak fluida berdasarkan data seismic dan sumur. Diharapkan dari hasil validasi berbagai macam atribut diharapkan dapat mendelineasi gambaran geologi yang kompleks ini.

Kombinasi dari atribut sweetness dan analisa AVO memperlihatkan distribusi dan orientasi dari target reservoir. Metoda ini membantu kita untuk menentukan tidak hanya kesuksesan sumur eksplorasi, tetapi diharapkan dapat memberikan ide untuk menambah kolam minyak yang ada. Karena dari studi inilah, resiko dari penentuan sumur development dapat secara signifikan berkurang.

## FOREWORD

I would like to express my gratitude to Allah SWT with His gift; I can accomplish my thesis project. And not forget prayer for Rasulullah Muhammad S.A.W and his family that always give us guidance until we become better person appropriate with Al-Quran and Hadists.

I realize that my thesis was not perfect, still need a lot of improvements. Therefore I apologize for all mistakes that may be found in this writing. Because of that reason, I opened opportunity to criticize and suggestion for this thesis project.

I would like to say thank you for:

1. Prof. Dr. Suprayitno Munadi as my supervisor, thank you for lectured knowledge and guidance in this thesis project.
2. All member Exploration and Development team of Musi Platform and Geoscience Technology member PT Medco E&P Indonesia, especially geophysical specialist team for the helped and coordination until I can finish my thesis work.
3. My classmate in University of Indonesia for giving me the wonderful time in the more last two years. I hope that us can become successful geoscientists that can applied our knowledge in appropriate.
4. The important part in the accomplishment in this thesis work is Ridwan Gumilar, my beloved future husband. Thank you Pan, to always giving me support. We hope this thesis project can make our future brighter.
5. And finally the most important part is my Family, for my parents and my little brother for the supported and prayed. It's give me power to accomplish my thesis writing.

I dedicate my thesis work to my family. Luv u all.

Jakarta, 3rd December 2009

## LIST OF CONTENTS

Approval Page.....	i
Abstract .....	ii
Abstrak .....	iii
Foreword .....	iv
List of Contents .....	v
List of Figures.....	vii
List of Attachments .....	xi
<b>Chapter 1. Introduction</b> .....	<b>1</b>
1.1 Background .....	1
1.2 Thesis Objective .....	1
1.3 Area .....	2
1.4 Hypothesis .....	2
1.5 Implication of the Study .....	3
<b>Chapter 2. Background Theory</b> .....	<b>4</b>
2.1 Regional Geology .....	4
2.1.1 Tectonic Setting .....	5
2.1.2 Stratigraphy .....	7
2.2 Petroleum System .....	11
2.2.1 Source Rock .....	11
2.2.2 Maturity .....	11
2.2.3 Reservoir .....	12
2.2.4 Seal .....	12
2.2.5 Hydrocarbon Play .....	12
2.3 Reservoir Characterization .....	14
<b>Chapter 3. Data and Methodology</b> .....	<b>16</b>
3.1 Input Data .....	16
3.1.1 Well Data .....	16
3.1.2 Seismic Data .....	16
3.2 Methodology .....	18

3.2.1 Sweetness Attribute .....	19
3.2.2 AVO .....	23
3.2.2.1 AVO Attributes and Techniques .....	25
3.2.2.2 Aki and Richard (1980) .....	28
3.2.2.3 AVO Classification by Rutherford and Williams .....	29
3.2.2.4 Bright Spot and Dim Spot .....	31
3.2.2.5 Limitations of thr AVO Method .....	33
<b>Chapter 4. Result and Discussion</b> .....	<b>36</b>
4.1 Data Preparation .....	36
4.1.1 Well Conditioning .....	37
4.1.2 Well Seismic Tie .....	35
4.1.3 Seismic Interpretation .....	41
4.2 Result of Fluid Substitution .....	43
4.3 Result of Sweetness Attribute .....	45
4.4 Result of AVO analysis .....	51
4.5 Analysis of Validation between Sweetness Attribute and AVO Analysis .....	55
<b>Chapter 5. Conclusions and Recommendations</b> .....	<b>58</b>
<b>References</b> .....	<b>60</b>
<b>Attachments</b> .....	<b>62</b>

## LIST OF FIGURES

<b>Figure 1.1</b> Map showing thesis area of Cantik Field, in Musi Platform area, South Sumatra Extension Block, Medco E&P operation area ...	2
<b>Figure 2.1</b> Regional Map of South Sumatra Basin (Kamal, 2008) .....	4
<b>Figure 2.2</b> Neogene-Paleogene Tectonic Framework Map of South Sumatra Basin (Kamal 2008) .....	5
<b>Figure 2.3</b> Geological Cross section west-east of South Sumatra Basin, showing the regional tectonic phase (Koesoemadinata, 2002, from Kamal 2008) .....	6
<b>Figure 2.4</b> Stratigraphic Coloumn of South Sumatra Basin (Kamal et, al., 2005) .....	7
<b>Figure 2.5</b> At least three cycles of the Baturaja carbonate development in the northeastern part of the Musi Platform can be recognized. With this technique, the stratigraphic position and lateral distribution of the basal clastic can be interpreted (Husni, 2005) .....	14
<b>Figure 3.1</b> Showing basemap of Cantik field.....	17
<b>Figure 3.2</b> Horizon slice from the top A-Sand showing instantaneous amplitude overlain on the depth contour map. The blue contour line represents the oil-water contact .....	21
<b>Figure 3.3</b> Horizon slice from top A-Sand showing the instantaneous frequency overlain on the depth contour structure map. The blue contour line represents the oil-water contact .....	22
<b>Figure 3.4</b> Horizon slice from top A-Sand showing sweetness overlain on the depth contour structure map. The pink circles represent eight new development wells. The blue contour line represents the oil-water contact. The correlation between low values of sweetness and high porosity .....	23
<b>Figure 3.5</b> Showing Ostrander model in thick sand filled by gas, gas in sand unit thickness of sand is very important to determining offset behavior (Ostrander, 1984) .....	26
<b>Figure 3.6</b> Showing Ostrander model in field data that contrasts amplitude	

with offset variation for gas-filled sands and sands without gas`..	27
<b>Figure 3.7</b> Superimposed an example of a Class IV gas sand on a figure taken from Rutherford and Williams which shows their gas-sand classification based on normal incidence reflection coefficient (Castagna et al., 1998)	31
<b>Figure 3.8</b> The AVO signatures of the corresponding seismic event would then be quite different	33
<b>Figure 3.9</b> Wedge model in which amplitude tuning occurs (Allen and Peddy, 1993)	35
<b>Figure 3.10</b> Highly porous water-wet sandstones can cause an increase in amplitude with offset similar to that caused by gas sands with lower porosity (Allen and Peddy, 1993)	35
<b>Figure 4.1</b> Well conditioning in F-4, showing log editing in density log and sonic log base on caliper, GR and SP analysis	36
<b>Figure 4.2</b> Showing crossplot result from depth and velocity data in F-2	38
<b>Figure 4.3</b> Showing wave extraction in well F-1, with parameter wavelet length 200 ms; taper length 25 ms and sample rate 2 ms	38
<b>Figure 4.4</b> Showing well seismic tie result in F-1, using wavelet F-1_PSTM, showing the 0.84 correlation result	39
<b>Figure 4.5</b> Showing 159° rotation phase in well F-1 makes the polarity in F-1 was reversed polarity	40
<b>Figure 4.6</b> Showing -18° rotation phase in well F-5 makes the polarity in F-1 was normal polarity	40
<b>Figure 4.7</b> Seismic section in wells location that showed seismic interpretation in Baturaja was depending by fluid content	41
<b>Figure 4.8</b> Show interpretation of Baturaja formation that possible because tuning effect	42
<b>Figure 4.8</b> Show seismic interpretation trespassing wells in Cantik field	43
<b>Figure 4.9</b> Show fluid substitution properties calculation window in well F-12	44



<b>Figure 4.10</b> Show fluid substitution result in well F-12, the black wiggle showed original seismic data, red wiggle showed fluid substitution replace by 100% gas and blue wiggle showed fluid substitution result replace by 100% wet .....	45
<b>Figure 4.11</b> Result Amplitude envelope in line 2905, Cantik field area, South Sumatra Basin .....	46
<b>Figure 4.12</b> Result Instantaneous Frequency in line 2905, Cantik field area, South Sumatra Basin .....	47
<b>Figure 4.13</b> Result sweetness attribute in line 2905, Cantik field area, South Sumatra Basin .....	48
<b>Figure 4.14</b> Result time slice sweetness attribute in time 950 ms, show interesting area in Cantik field area, South Sumatra Basin ..	49
<b>Figure 4.15</b> Overlay bubble map from water cut data and interesting area in Cantik field area, South Sumatra Basin .....	49
<b>Figure 4.16</b> Result amplitude map in top of Baturaja Formation, show possibility of fluid content in Cantik field area, South Sumatra Basin .....	50
<b>Figure 4.17</b> Result horizon slice sweetness attribute in top of Baturaja Formation, show more possibility of fluid content in Cantik field area, South Sumatra Basin .....	51
<b>Figure 4.18</b> Super gather sections in arbitrary line trespassing wells in Cantik Field .....	52
<b>Figure 4.19</b> Angle gather section in arbitrary line trespassing wells in Cantik Field .....	52
<b>Figure 4.20</b> Crossplot result from well F-12, see the relationship result from fluid content, yellow was gas area; blue was oil area and red was water area .....	53
<b>Figure 4.21</b> AVO result product A*B in arbitrary line trespassing wells in Cantik Field .....	54
<b>Figure 4.22</b> AVO result Intercept (A) in arbitrary line trespassing wells in Cantik Field .....	55

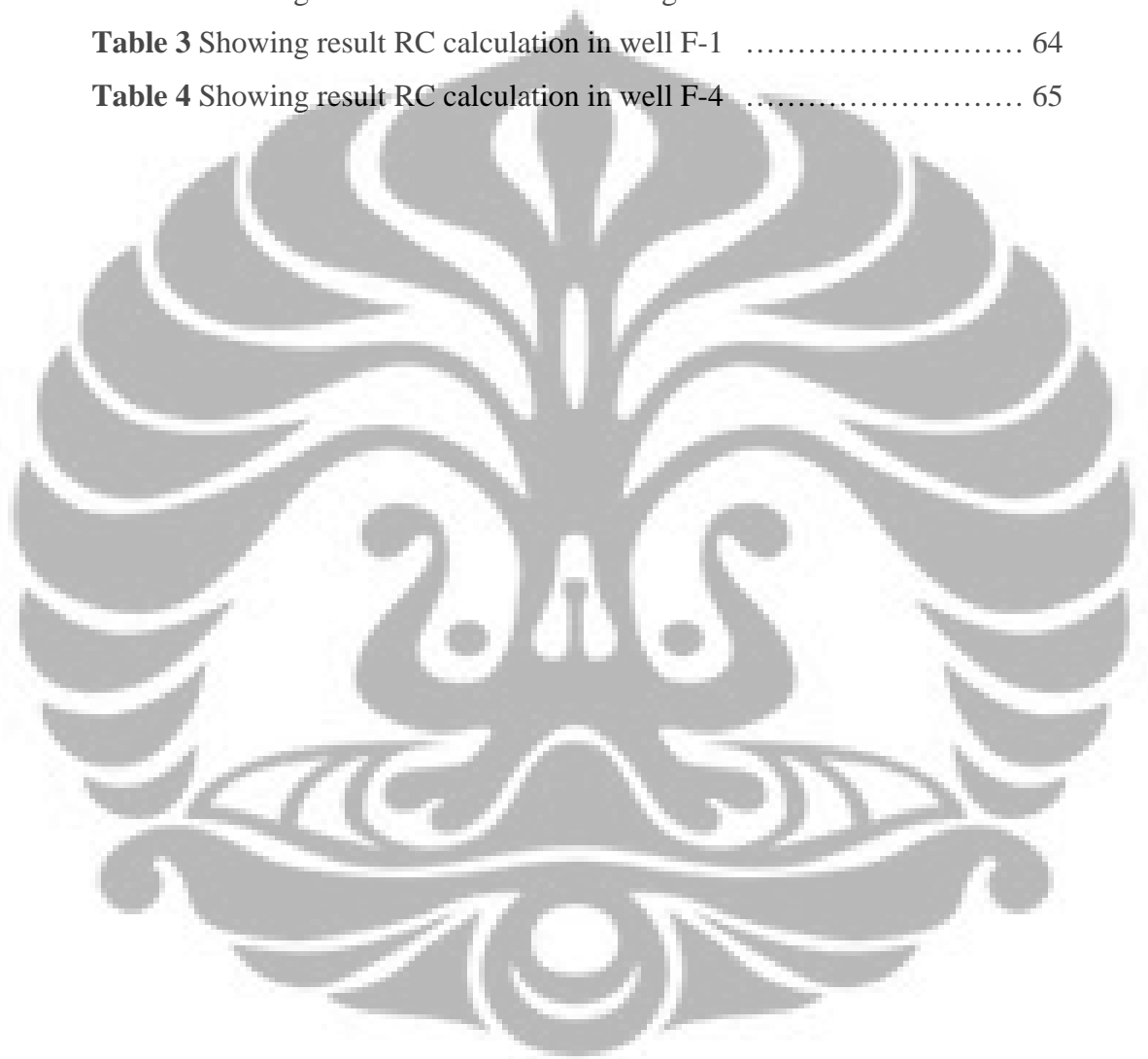
**Figure 4.23** AVO result Intercept (B) in arbitrary line trespassing wells  
in Cantik Field ..... 55

**Figure 4.24** Sweetness result that show interesting area in the flank ..56



## LIST OF ATTACHMENTS

<b>Table 1</b> Table 1 Showing the checkshot data and calculating result of velocity based on checkshot data, the red column showed negative velocity .....	62
<b>Table 2</b> Showing result after checkshot editing .....	63
<b>Table 3</b> Showing result RC calculation in well F-1 .....	64
<b>Table 4</b> Showing result RC calculation in well F-4 .....	65



# Chapter 1

## INTRODUCTION

### 1.1 Background

Cantik is an oil-producing field located in South Sumatra Extension Block, a Medco E&P operation area. Cantik has 10 oil producer wells. Oil in-place volumetric calculations predict approximately 4.2 MMBO, while the proven reserve is about 1.3 MMBO. From the two last drillings founded that the reservoir was tight and difficult to develop. From that point make bigger challenges to develop Cantik field with a new approach method.

In 1980 until 1990, oil that produced usually was in sandstone reservoir. For carbonate reservoir need unconventional attribute and advance interpretation methods (Brown, 1996). Conventional attribute and interpretation methods provide limited access for delineating a highly heterogeneous reservoir distribution. Due to the problems of heterogeneous limestone and complex stratigraphic trap interpretation, it is difficult to develop and manage Cantik field. Conventional attributes that usually used in limestone reservoir has limited. Heterogeneity properties of carbonates were difficult to detect. Approach method that usually was done is about fluid content. Fluid effect in seismic section was easier to define in carbonates. In this study we tried to make validation of various attribute that have relationship in fluid content or fluid contact. Hopefully with that method can help us to make decision next development wells.

### 1.2 Thesis Objective

Objective of this thesis was compared between various methods that related to find reservoir properties, especially in fluid relation. Various methods that we used were sweetness attribute and AVO analysis. Challenge from this thesis was how to compare various methods that have different result. Sweetness attribute were defined carbonate-shale ratio and also fluid content. And from AVO analysis we can find fluid contact distribution. The combination of sweetness attribute and AVO model reveals the distribution and orientation of the

University of Indonesia

reservoir targets and fluid contact, which are consistent with well data. This method helped us to propose not only successful exploration wells but also gave us an idea about the extent of the pool. We hope from this study, the risks of proposing development wells can significantly be reduced.

### 1.3 Area

Cantik is an oil-producing field located in Musi Platform, South Sumatra Extension Block, a Medco E&P operation area. Cantik has 10 oil producer wells, which is producing from Baturaja Formation (Figure 1.1). From oil in-place volumetric calculations predict approximately 4.2 MMBO, while the proven reserve is about 1.3 MMBO. And for gas reserve it will be produce in 2015. Before 2015, we hope the target reserve from oil producing can be success, so we need advance study to develop this field.

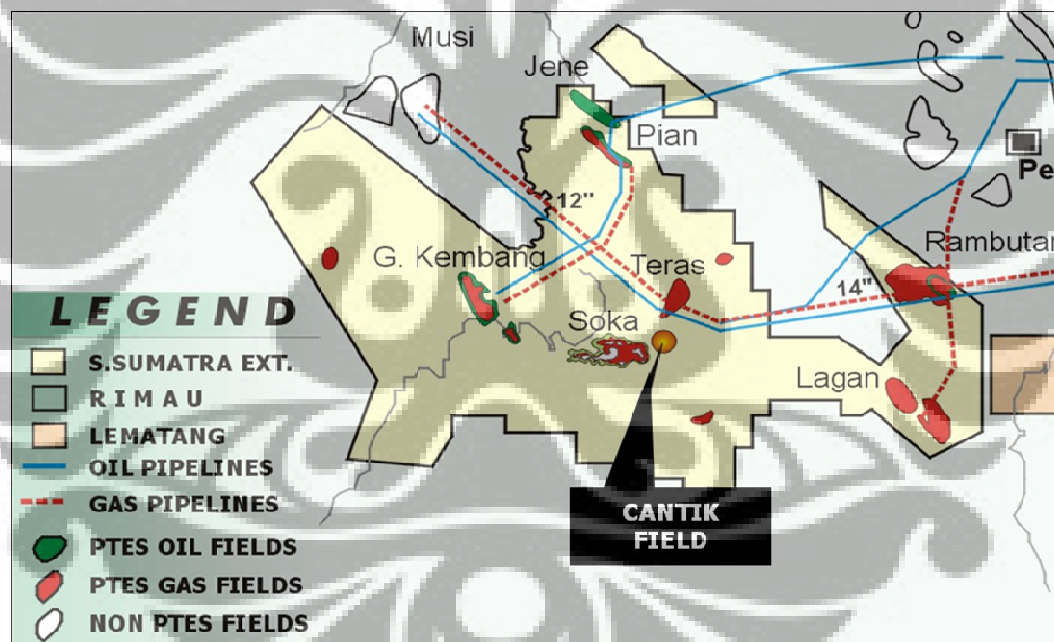


**Figure 1.1** Map showing thesis area of Cantik Field, in Musi Platform area, South Sumatra Extension Block, Medco E&P operation area

### 1.4 Hypothesis

A fully integrated multidisciplinary approach to interpretation, characterization, and porosity modeling in 3-D seismic data is essential to accurate and timely results for exploitation success (Brown, 1996). From the

University of Indonesia

conventional interpretation in stacking data seismic, we have difficulties to define reservoir distribution. From condition of high frequency seismic distribution, we hope we can find the laterally distribution of Baturaja Formation in Cantik Field. The characterization from various attribute can make simulation about reservoir characterization especially from physical character like lithology and also fluid content in seismic data. All of validation from various parameter results can increase the confidence level to predict quantitatively reservoir character in Baturaja Formation of Cantik Field.

### **1.5 Implication of the Study**

The integration of well log data and various seismic attributes response will guide the interpretation and give an ever increasing confidence that the model can be used to drive reservoir distribution model in the Cantik Field. This study is potentially resolves ambiguities between different types of parameter scenario and determines the porous oil and gas reservoir distribution through seismic data based on well data which is validated from well log data. Development and application of this integrated methodology were no less important a result than the well recommendations. However, the fundamental three-part simplicity of the integration process (interpretation, characterization, and simulation) is important to emphasize in light of numerous ancillary procedures. An additional conclusion from this thesis, then, is the importance for geosciences staff members to continue their work beyond basic workstation interpretation.

## Chapter 2

### BACKGROUND THEORY

#### 2.1 Regional Geology

The South Sumatra Basin is located to the east of the Barisan Mountains and extends into the offshore areas to the northeast and regarded as a back-arc basin, which is bounded by Barisan Mountains to southwest and the pre-Tertiary of the Sunda Shelf to the northeast (de Coster, 1974) (Figure 2.1). The South Sumatra Basin was formed during east-west extension at the end of the pre-Tertiary to beginning of tertiary times (Daly et al., 1987 From Kamal 2008). Orogenic activity during the Late Cretaceous to Eocene cut the basin into four sub-basins.

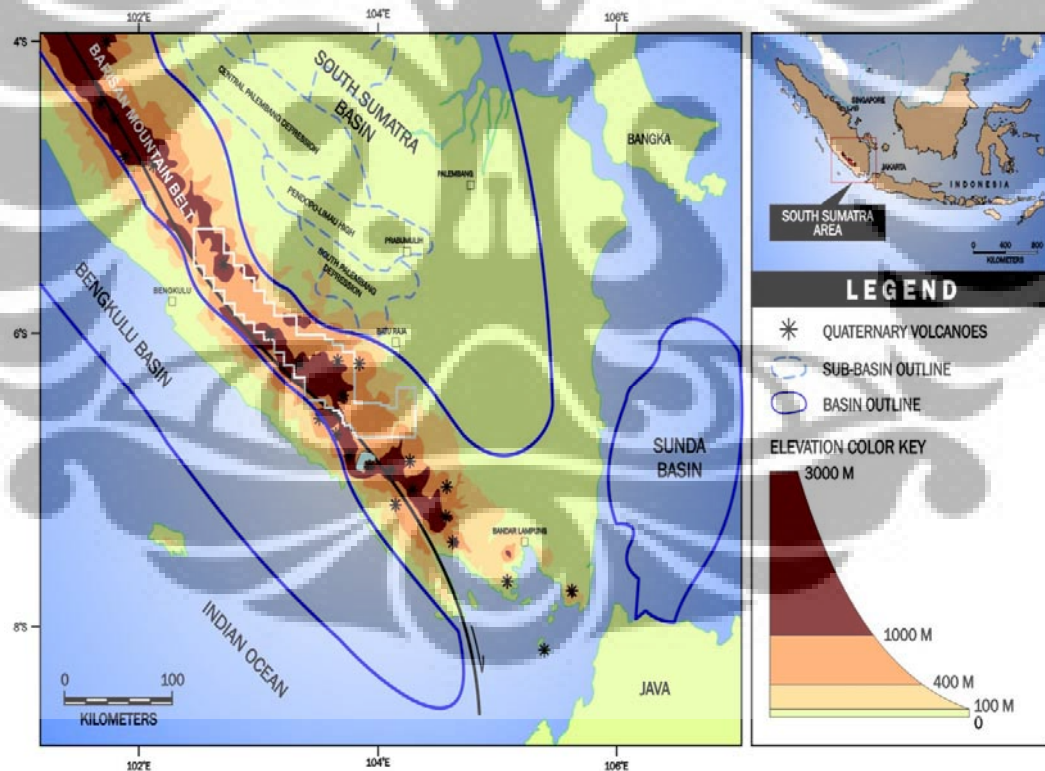


**Figure 2.1** Regional Map of South Sumatra Basin (Kamal, 2008)

### 2.1.1 Tectonic Setting

The present day structural style of the South Sumatra Basin is consequence of three major episodes (Figure 2.3):

- 1) Northeast to southwest and north to south trending horst blocks and half grabens be formed during an initial extensional period from the latest Cretaceous to Early Oligocene resulted from complex plate readjustment as a consequence of collision of India with Asia (Figure 2.2).. Sedimentation at this time consisted predominantly of coarse clastics and volcanoclastics within predominantly continental/lacustrine environments

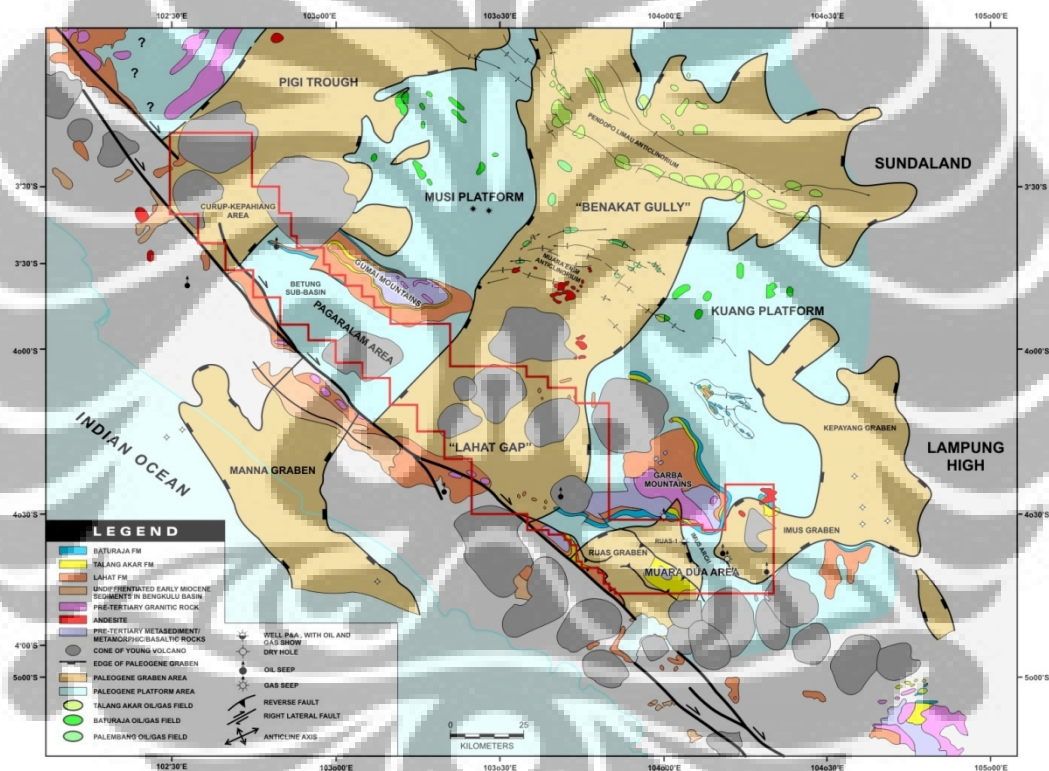


**Figure 2.2** Neogene-Paleogene Tectonic Framework Map of South Sumatra Basin  
(Kamal 2008)

- 2) Graben subsidence continued through a tectonically quiescent period from Late Oligocene through Early Miocene time when the basin became fully marine. During Late Early to Middle Miocene time wrench tectonics produced compressional folds due to the oblique subduction of the oceanic plate southwest of Sumatra



- 3) Finally during the Plio-Pleistocene strong compressional tectonics associated with uplifting of the volcanic arc to the west reactivated earlier structural feature and created northwest-southeast trending reverse faults and basement uplift

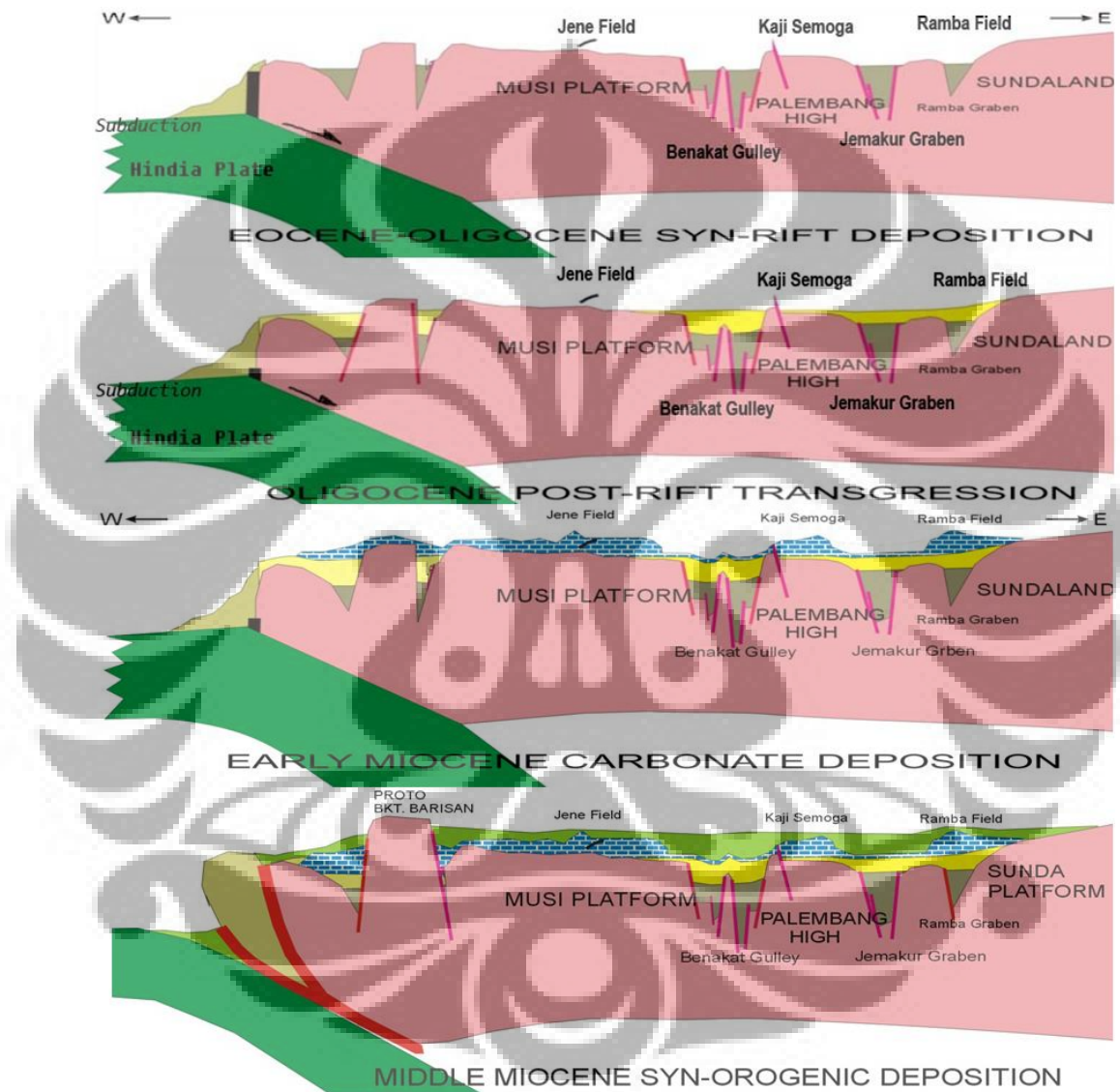


**Figure 2.3** Geological Cross section west-east of South Sumatra Basin, showing the regional tectonic phase (Koesoemadinata, 2002, from Kamal 2008)

## 2.1.2 Stratigraphy

Stratigraphy in South Sumatra Basin was control by process of megacycle system of transgression and regression sedimentation in regionally, just like sedimentation in west Indonesia (Figure 2.4).

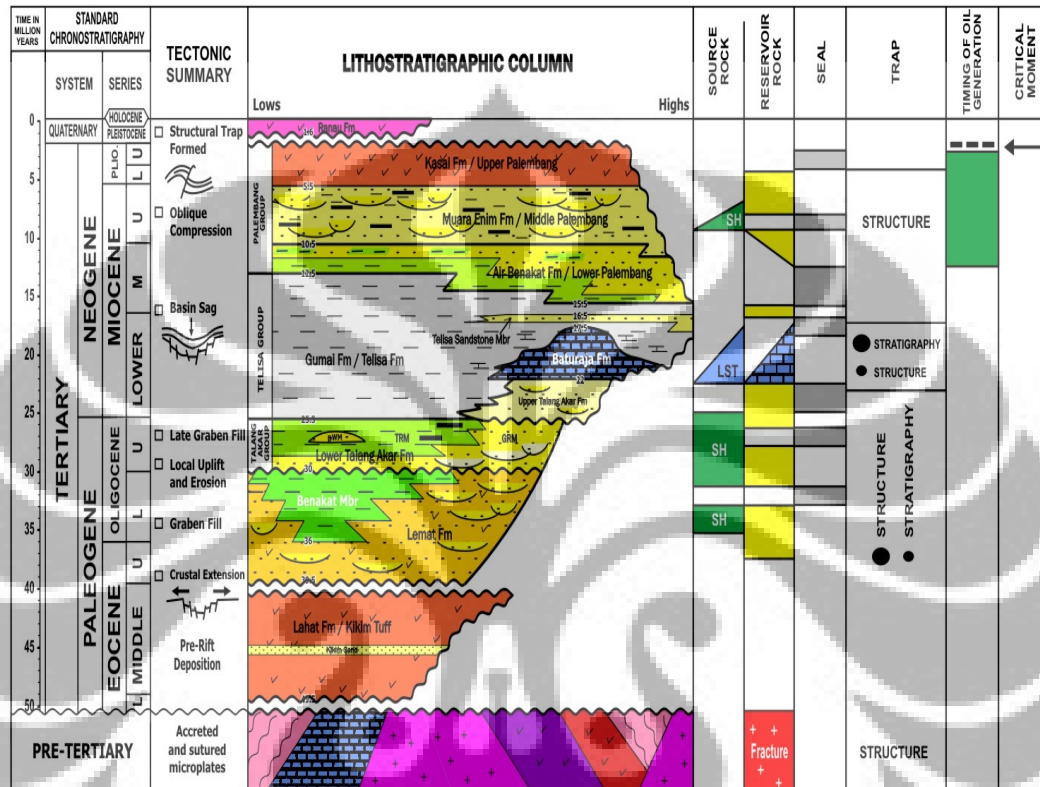


Figure 2.4 Stratigraphic Column of South Sumatra Basin (Kamal et. al., 2008)

### 1) Cretaceous

The complexly folded Pre-Tertiary in the Gumai Mountains contains two different units, the relations of which are unclear:

- Saling Formation: Mainly poorly bedded volcanic breccias, tuffs and basaltic-andesitic lava flows, hydrothermally altered to greenstones. The Saling Formation rocks may be a Late Jurassic-Early Cretaceous volcanic island arc association with fringing reefs.
- Lingsing Formation: Mainly grey-black, thin-bedded shales or slates, with minor interbeds of green andesitic-basaltic rock, radiolarian-bearing chert

and several tens of meters thick limestone bed rich in the Early Cretaceous foraminifer *Orbitolina*, but without corals. The Lingsing Formation rocks suggest an Early Cretaceous deep-water facies.

## 2) Tertiary

### a. Lahat Formation (Musper, 1973, from Kamal 2008)

The Lahat volcanics unconformable overlying the Pre-Tertiary, but conformable under "Talang Akar" and Baturaja sediments is a thick (up to 3350m) series of andesitic volcanic breccias, tuffs, lahar deposits and lava flows, with a remarkable quartz-sandstones horizon in the middle. The formation is possibly an equivalent to the widespread "Old Andesites" of Sumatra and Java. On Java these are dated as the Oligocene, overlying marine Middle and Late Eocene beds.

Three members of the Lahat Formation are distinguished; from old to young are Lower Kikim Member, Quartz-sandstone Member and Upper Kikim Member. The Lahat Formation underlies the Talang Akar Formation and consist of fluvial or alluvial fan sands, lacustrine and fluvial clays and coals and it are questionable whether these are the same as the Lahat volcanic.

### b. Pre-Baturaja Clastics

In the South Sumatra basin a highly variable complex of clastic sediments is found between the Lahat volcanic and the Early Miocene marine Baturaja or Telisa Formations. The basal part with volcanoclastic sediments and lacustrine clays is called Lemat Formation, and is either a distal facies of the Lahat Formation or, more likely, a younger unit rich in debris from the Lahat Formation. The upper part of the graben-fill series is the fluvial and deltaic Talang Akar Formation, which is mainly Late Oligocene age.

### c. Baturaja Formation

Limestones that found in various places near the base of the Telisa Formation are usually attributed to the Baturaja Formation. It is locally

developed shallow water facies of lower Telisa shales and should probably be regarded as a member of this formation. Both massive reefal facies and deeper water fine-grained well-bedded limestones with thin marl intercalations are present. The age of this formation is within the lower part of the Early Miocene (Upper Te Letter Stage, equivalent to planktonic foraminifera zones N5-N6)

d. Telisa Formation/Gumai Formation (Tobler 1906, from Kamal 2008)

Telisa formation is characterized by a thick series of dark grey clays, usually with common planktonic foraminifera that may form thin white laminae. Whitish tuffs and brown turbiditic layers that composed of andesitic tuffaceous material are locally common. Layers with brown, lenticular calcareous nodules up to 2m in diameter are most common in the upper part of the formation.

The age of the formation is variable. The place where no Baturaja limestone is developed, the basal Telisa beds is zone N-4 planktonic foraminifera (lower Early Miocene). The place where Baturaja is thick, oldest Telisa beds is zone N6 or N7 (Early Miocene). The age of the top Telisa Formation also varies, from zone N8 (upper Early Miocene) to zone N10 (Middle Miocene), depending on position in the basin and where the formation boundary is picked.

e. Palembang Formation (Air Benakat, Muara Enim and Kasai Formations)

This formation is the “regressive” stage of the South Sumatra basin fill. Facies show an overall shallowing-upward trend from predominantly shallow marine at the base; through coastal deposits to fluvial beds in the top member. In detail the formation is composed of numerous thin transgressive-regressive para-sequences.

Three Members are distinguished:

- Lower Palembang Member (Air Benakat Fm.)

The Air Benakat Formation consists of predominantly shales interbeds with siltstones, sandstones and limestones. The thickness of the

formation is ranging from 100m to 1000m. the age of the formation is Middle Miocene, possibly ranging up into the Late Miocene.

- Middle Palembang Member (Muara Enim Fm.)

The top and bottom of this unit are defined by the upper and lower occurrence of laterally continuous coal beds. The thickness in the area around Muara Enim and Lahat is around 500-700m, about 15% of which is coal. The part where the mwmbwer is thin, coal beds become very thin or are absent. This fact suggests that subsidence rates played an important role in coal deposition and preservation. The age of member has never been determined accurately, however, it should be within the Late Miocene-Early Pliocene.

- Upper Palembang Member (Kasai Fm.)

The lithology of the Kasai Formation comprises pumice tuffs, tuffaceous sandstones and tuffaceous claystones. The depositional facies are fluvial and alluvial fan with frequent ashfalls (non-andesitic). Fossil are rare, only some fresh-water mollusks and plant fragments are available (Musper, 1933; 1937). The most likely, the age is Late Pliocene to Pleistocene.

### 3) Quaternary

The Quaternary rocks is possibly unconformable overlie Palembang or older formations, and could usually be distinguished from Palembang beds by the presence of dark-colour and esitic and basaltic volcanic rocks.

Other rocks included: in this Quaternary are the "liparites" (ignimbrites) filling valleys in the Pasumah region south of the Gumai Mountains, the andesitic tuffs and lahars in the Pasumah region derived from Barisan volcanoes like Dempo, and terrace deposits along the major rivers.

## 2.2 Petroleum System

### 2.2.1 Source Rock

The principal source rocks in the South Sumatra Basin are fluvio-deltaic marine, locally lacustrine and coaly facies of the Late Eocene to Middle Oligocene Lemat, and Late Oligocene to Early Miocene Talang Akar Formations. These rocks were deposited in the grabens and half grabens forms during the Late Cretaceous to Early Oligocene, and contribute to terrestrial derived oils. In addition, shales of the Telisa Formation provide a marine/paralic hydrocarbon source.

The Talang Aka rang Lemat lithologies are dominated by a coaly facies and have excellent source rock potential with TOC values greater than 3% and HI values greater than 300. Potential source rock facies are dominated by type II/III kerogens derived from higher plant material, with minor leptinite, algal and exinite component.

### 2.2.2 Maturity

The average geothermal gradient in the South Sumatra Basin is 2.89 degree F per 100 feet. Assuming an oil generation threshold of 250 degree F, average depth to the top of oil window in South Sumatra Basin is 1700 meters (5600 feet). Assuming a gas generation threshold of 300 degree F, average depth to the top gas window is approximately at 2300 meters (7300 feet).

Generation of hydrocarbon from Lemat and Talang Akar Formations probably began in the Late Miocene, governed by heat flow increase associated with Late Miocene tectonics, and entered the gas window in Pliocene or Late Pliocene time. Early trapped hydrocarbon may also have re-migrated following the Pliocene-Pleistocene orogeny.

### 2.2.3 Reservoir

The main oil and gas producer in South Sumatra Basin is the Eocene-Oligocene sandstones of the Talang Akar Formation, carbonate reef of Baturaja Formation and sandstones of Air Benakat Formation.

The sandstones series of Talang Akar are developed in lower part of this formation, which consist of quarts as the result of metasediment rock leaching. The porosity is 18% to 30%. The carbonate rocks of Baturaja Formation could be divided into two (2) groups such as the lagoon facies is dominated by large benthic foraminifer with wackstones texture, and the reefal facies consists mainly of coral, red algal, mollusks, large benthonic foraminifer that built in wackstones or packstones.

The Early Miocene Gumai sandstones are also proved as main oli and gas in the South Sumatra Basin.

### 2.2.4 Seal

Intraformational shales and claystones within the Talang Aka rang Gumai Formations provide the main seal for reservoir targets; as a result fields will typically have stacked reservoirs with multiple fluid contacts. The Lower Gumai shales can act as regional seal for the older reservoir targets (Talang Akar sandstones and possible Baturaja limestones). Air Benekat Formation is considered as a poor seal since it mainly consists of sands and silts.

### 2.2.5 Hydrocarbon Play

Talang Akar sandstones constituted the main reservoir target and the potential traps are anticlinal structure that developed in response to Plio-Pleistocene compression. The Baturaja limestones are the other prime reservoir target; the traps are structural or combined structural and stratigraphic trap potential has also been indentified in the Baturaja Formation, with the potential trap dependent on facies change from porous reefal to tight platform carbonates

The Lower Palembang sandstones could represent an additional target in the South Sumatra Basin. The play is structural; with Lower Palembang Formation occurring at a depth of less than 2,000 ft. Thick regional shales of the Gumai Formation provide the top seal. An intra-formational seal could also be present in transitional geological settings between non-marine and shallow marine where the Baturaja carbonates begin to develop. Seal risk may also occur where porous Baturaja limestone onlaps directly onto basement. If the limestone is thin and tight but is associated with highly fractured and porous basement, hydrocarbons might also not be trapped in the basal clastic reservoir.

The dominant trap in the Cantik Field is structural. Further analysis of variation of the trapping styles is still needed. The updip stratigraphic pinch-out maybe an attractive play that has not yet been fully investigated (Figures 2.5). The productive mature source rocks for existing plays in the Musi Platform are shales of the Lemat and Talang Akar Formations located in the Pigi Trough approximately 10 km to the northwest and Benakat Gully approximately 15 km to the east.

The main hydrocarbon migration pathway from the sources into the Baturaja limestone and pre-Tertiary fractured basement reservoirs is interpreted to be through the basal clastics. Migration along fault conduits may not be significant since the influence of Plio-Pleistocene tectonics is minor. Potential areas to search for this play are the flanks of paleo-basement complexes and regional pinchouts towards the southwest where the marine shelf shales and/or tight platform carbonates become the updip lateral seal which prevent re-migration to the southwest following tilting of the Musi Platform. Possible unrecognized sedimentary plays could also be present along the flank of the platform. Concepts to explore the play further are still being developed.



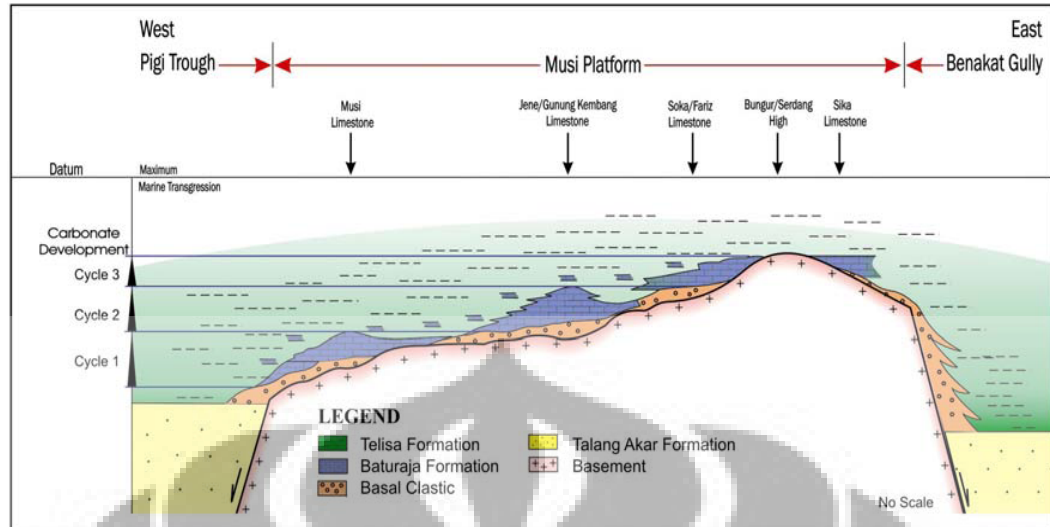


**Figure 2.5** At least three cycles of the Baturaja carbonate development in the northeastern part of the Musi Platform can be recognized. With this technique, the stratigraphic position and lateral distribution of the basal clastic can be interpreted (Husni, 2005)

## 2.1 Reservoir Characterization by Attributes Seismic

Seismic Attributes are all the information obtained from seismic data, either by direct measurements or by logical or experience based reasoning (Tanner, 2002). Based on their definition, the computation and the use of attributes go back to the origins of seismic exploration methods. The arrival times and dips of seismic events were used in geological structure estimation. Frank Rieber in the 1940's introduced the Sonograms and directional reception (Tanner, 2002). This method was extensively used in noise reduction and time migration. The introduction of auto-correlograms and auto-convolograms (Anstey and Newman, from Tanner 2002) led to better estimates of multiple generation and more accurate use of the later developed deconvolution. NMO velocity analysis gave better interval velocity estimates and more accurate subsurface geometries. Bright spot techniques led to gas discoveries, as well as to some failures. This was improved by the introduction of AVO technology. Each of these developments has helped our understanding of the subsurface and reduced the uncertainties.

Unfortunately, one of the principal failures of any of the individual techniques was our implicit dependence on it. Finally, the power of the combined use of a number of attributes is being recognized and successful techniques are being introduced. The attribute discussed is the outcome of the work relating to the combined use of several attributes for lithology prediction and reservoir characterization.

Complex seismic trace attributes were introduced around 1970 as useful displays to help interpret the seismic data in a qualitative way. Walsh of Marathon published the first article in the 1971 issue of *Geophysics* under the title of "Color Sonograms". At the same time Nigel Anstey of Seiscom-Delta had published "Seiscom 1971" and introduced reflection strength and mean frequency (Tanner 2002). He also showed color overlays of interval velocity estimates for lithological differentiation. The new attributes were computed in the manner of radio wave reception. The reflection strength was the result of a low pass filtered, rectified seismic trace. The color overlays showed more information than was visible on the black and white seismic sections. Realizing the potential for extracting useful instantaneous information, Taner, Koehler and Anstey turned their attention to wave propagation and simple harmonic motion. This led to the recognition of the recorded signal as representing the kinetic portion of the energy flux. Based on this model, Koehler developed a method to compute the potential component from its kinetic part. Dr. Neidell suggested the use of the Hilbert transform. Koehler proceeded with the development of the frequency and time domain Hilbert transform programs, which made possible practical and economical computation of all of the complex trace attributes. In the mid 70's three principal attributes were pretty well established. Over the years a number of others were added.

The study and interpretation of seismic attributes give some qualitative information of the geometry and the physical parameters of the subsurface. It has been noted that the amplitude content of the seismic data is the principal factor for the determination of physical parameters, such as the acoustic impedance,

reflection coefficients, velocities, absorption etc (Hart, 2004). The phase component is the principal factor in determining the shapes of the reflectors, their geometrical configurations etc. Attributes discuss the several computational methods of conventional attributes, basically the computation of the analytic trace. In the second part attributes present computation of the conventional attributes and their derivatives. One point that must be brought out is that we define all seismically driven parameters as the Seismic Attributes. They can be velocity, amplitude, frequency, rate of change of any of these with respect to time or space and so on. Attributes classification is based on their computational characteristics. They can be computed from pre-stack or post stack data sets. Some of the attributes computed from the complex trace such as envelope, phase etc. correspond to the various measurements of the propagating wave front, its call as the 'Physical Attributes'. Others computed from the reflection configuration and continuity is call as 'Geometrical Attributes'. The principal objectives of the attributes are to provide accurate and detailed information to the interpreter on structural, stratigraphic and lithological parameters of the seismic prospect.

## Chapter 3

### DATA AND METHODOLOGY

#### 3.1 Input Data

##### 3.1.1 Well Data

Cantik Field has 15 wells and 1 trajectory well (Figure 3.1). From 16 wells in Cantik field only 2 wells that have information of shear wave for identification of rock properties, they are: F-11 and F-12. Calibration and validation of various attribute is concern in all of wells data. For checkshot survey is required in 2 wells that are in F-1 and F-2. Checkshot survey is required for time depth conversion and well seismic tie, while production test data is required to be input as reservoir properties in fluid substitution method.

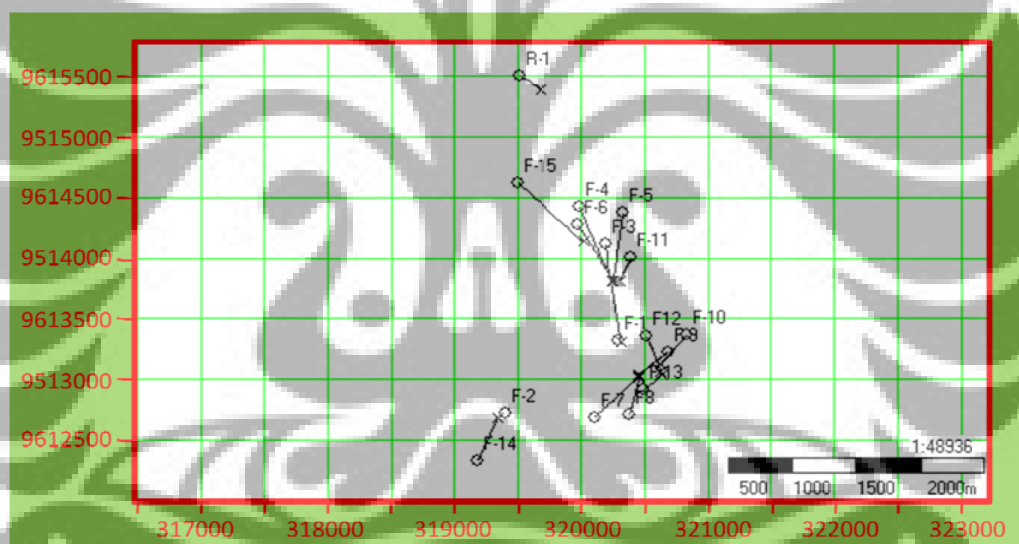


Figure 3.1 Showing basemap of Cantik field

##### 3.1.2 Seismic Data

The seismic data used in this study is Pre Stack Depth Migration, Post Stack Time Migration and gather Post Stack Time Migration. The seismic data is from 2006. Total swath for this project is 16 with 15521 records. The data coverage of these surveys is about 120 square kilometers. The survey acquired using receiver line spacing 225 meters and shot line spacing 500 meters. The

orientation of receiver line is 90 degrees and 135 degrees for source line. Shot point spacing is 35.4 meters and receiver point spacing is 25 meters. The survey was processed using a sample interval 2 ms and record length 4 seconds. The processing sequence included the application of spherical spreading correction, 3D refraction static, 3D surface consistent Deconvolution, 3D sorting, 3D surface consistent residual static, Pre Stack Time Migration. The final migrated volume data consists of 3D coverage with a 12.5 meter by 12.5-meter grid.

The area is limited by inline 2002-3045 and crossline in 10000-11700. But for gather data is only in spot area. PSTM gather in Cantik Field is not complete, because they have problem in database management. Gather that in used is surrounding of wells area and in prospect area.

### **3.2 Methodology**

The initial objective was to develop as many physical attributes as possible in order to define the lithological parameters and reservoir characteristics from different points of view. In the development we established a general classification of attributes based on their input data and their usage. Attributes can be computed from pre-stack or from post-stack data before or after time migration. The procedure is the same in all of these cases. Attributes can be classified in many different ways (Brown, 1996). Computationally Tanner divide attributes into two general classes.

- a) Class I attributes are computed directly from traces. This data could be pre- or post-stack, 2-D or 3-D, before or after time migration. Trace envelope and its derivatives, instantaneous phase and its derivatives, bandwidth, Q, dips etc. are some of the attributes computed this way.
- b) Class II attributes are computed from the traces with improved S/N ratios after lateral scanning and semblance-weighted summation. Details of the computation are given in the Maximum Semblance Computation section of the Geometrical attributes. All of the Class I attributes are computed in Class II. In addition lateral continuity and dips of maximum semblance are computed from the scanning procedure.

Another classification is based on the relation of the attributes to the geology:

- a) Physical attributes relate to physical qualities and quantities. The magnitude of the trace envelope is proportional to the acoustic impedance contrast, frequencies relate to the bed thickness, wave scattering and absorption. Instantaneous and average velocities directly relate to rock properties. Consequently, these attributes are mostly used for lithological classification and reservoir characterization.
- b) Geometrical attributes describe the spatial and temporal relationship of all other attributes. Lateral continuity measured by semblance is a good indicator of bedding similarity as well as discontinuity. Bedding dips and curvatures give depositional information. Geometrical attributes were initially thought to help the stratigraphic interpretation. However, further experience has shown that the geometrical attributes defining the event characteristics and their spatial relations, quantify features that directly help in the recognition of depositional patterns, and related lithology.

Most of the attributes, instantaneous or wavelet is assumed to study the reflected seismic wavelet characteristics. That is, we are considering the interfaces between two beds. However, velocity and absorption are measured as quantities occurring between two interfaces, or within a bed. Therefore, we can divide the attributes into two basic categories based on their origin. Attributes is corresponding to the characteristics of interfaces. All instantaneous and wavelet attributes can be included under this category. Pre-stack attributes such as AVO are also reflective attributes, since AVO studies the angle dependent reflection response of an interface.

### 3.2.1 Sweetness Attribute

Seismic attributes can be broadly categorized into three classes namely- horizon based attributes, sample based attributes and stratal-based attribute. Horizon based attributes are calculated within a specified time window. Horizon based attributes include coherency type attribute, ratio type and averaged

attributes. Sample based attributes are calculated at a particular time of interest. Stratal amplitudes are a special type of horizon amplitudes. In specific zones within the horizons where it is difficult to track a particular event in the seismic data several strata are created within the horizon of interest. The strata follow the upper or lower horizons or are an average between the two. Depending upon the coherency of the amplitude strength within the zones several attributes can be developed for each of the strata (Mukherje, 2008, from Brown 1996).

Case study that have already implementation of sweetness attribute become one of method to define the reservoir and fluid content distribution is in SWB Field, base on Sigit Sukmono et al paper (2008). Instantaneous amplitude or reflection strength is a complex attribute that measures the total energy of the seismic signal at a specific instant of time. It can therefore be seen as amplitude that is independent of phase. It serves as the envelope of the seismic trace for every time sample. The values of instantaneous amplitude are always positive with magnitudes close to that of the real data. Sharp changes in instantaneous amplitude are often associated with a sharp change in lithology. This can occur at an unconformity boundary or at a sharp change in depositional environment. Figure 3.2 shows that large instantaneous amplitudes are associated with large values of net pay and porosity.

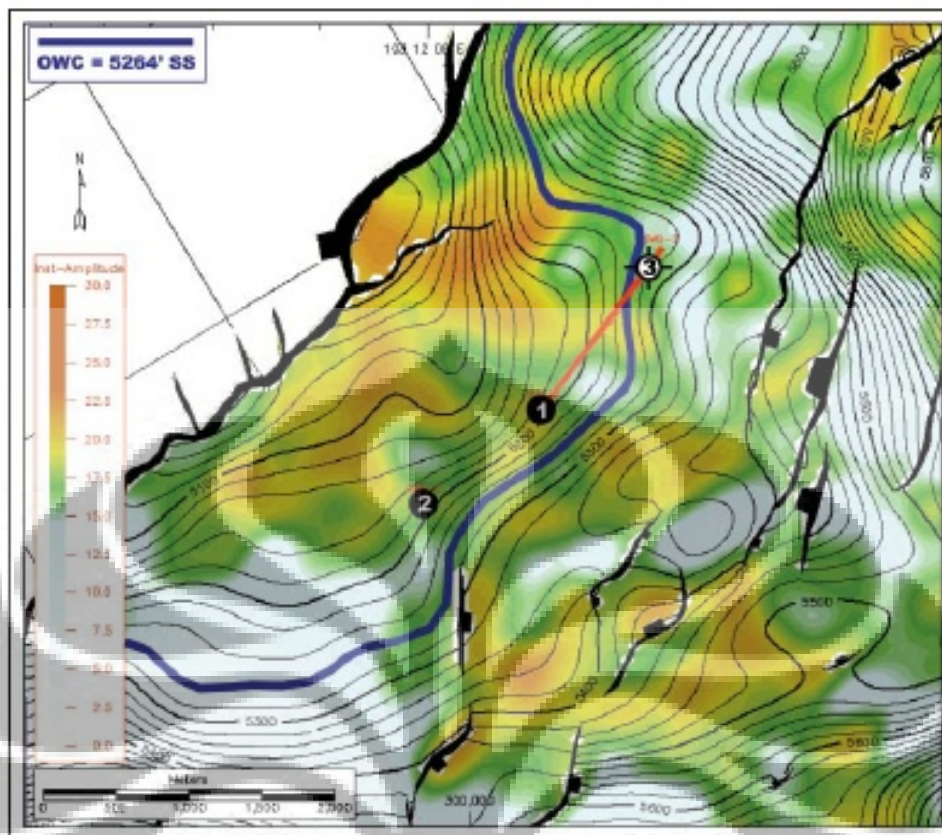


Figure 3.2 Horizon slice from the top A-Sand showing instantaneous amplitude overlain on the depth contour map. The blue contour line represents the oil-water contact.

Instantaneous frequency, another complex attribute, measures the time rate of phase changes and provides information on the frequency of reflector packages. In this case, high porosity and thicker deposits are associated with lower instantaneous frequency (Figure 3.3).



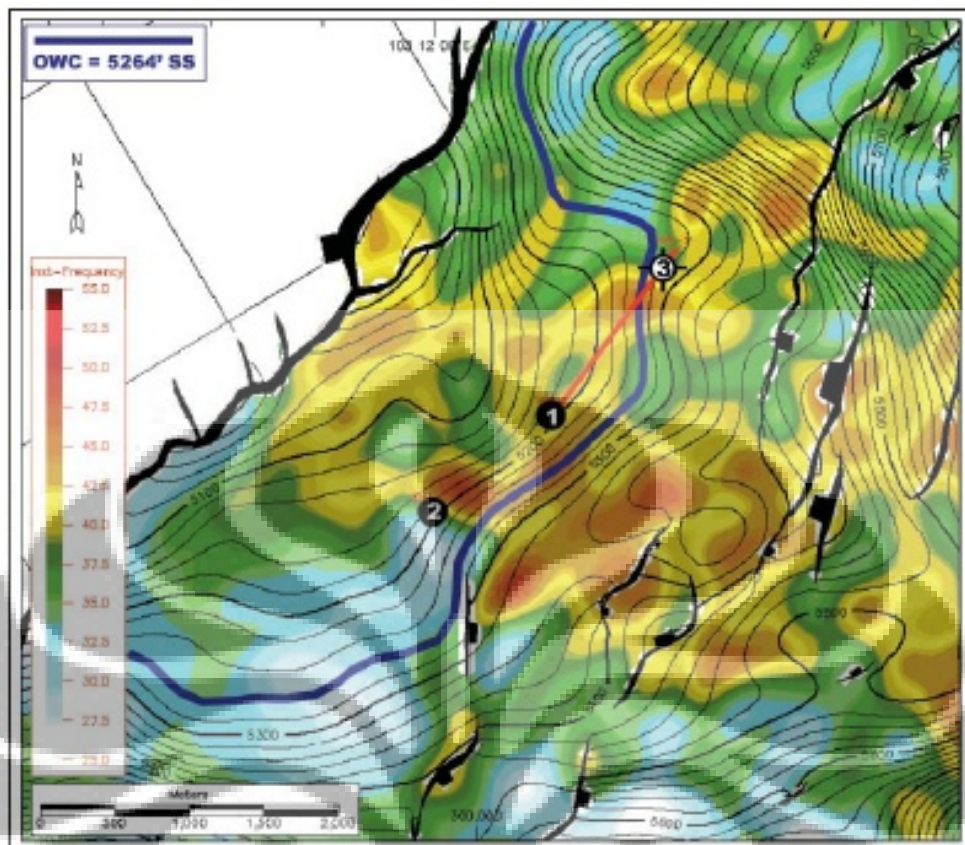


Figure 3.3 Horizon slice from top A-Sand showing the instantaneous frequency overlain on the depth contour structure map. The blue contour line represents the oil-water contact.

The sweetness attribute enhances the contrast between areas having subtly different net pay and porosity values when mapped using other attributes. High values of net pay and porosity are shown to be associated with lower sweetness values (Figure 3.4). Horizon slices of SNA, instantaneous amplitude, instantaneous frequency, and sweetness (Figures 3.2 – 3.4) give similar patterns. The distribution of high net pay and porosity is constrained to the middle part of the study area and oriented NW-SE. As expected, the sweetness map shows the sharpest contrast between the high and low values of porosity and netpay.

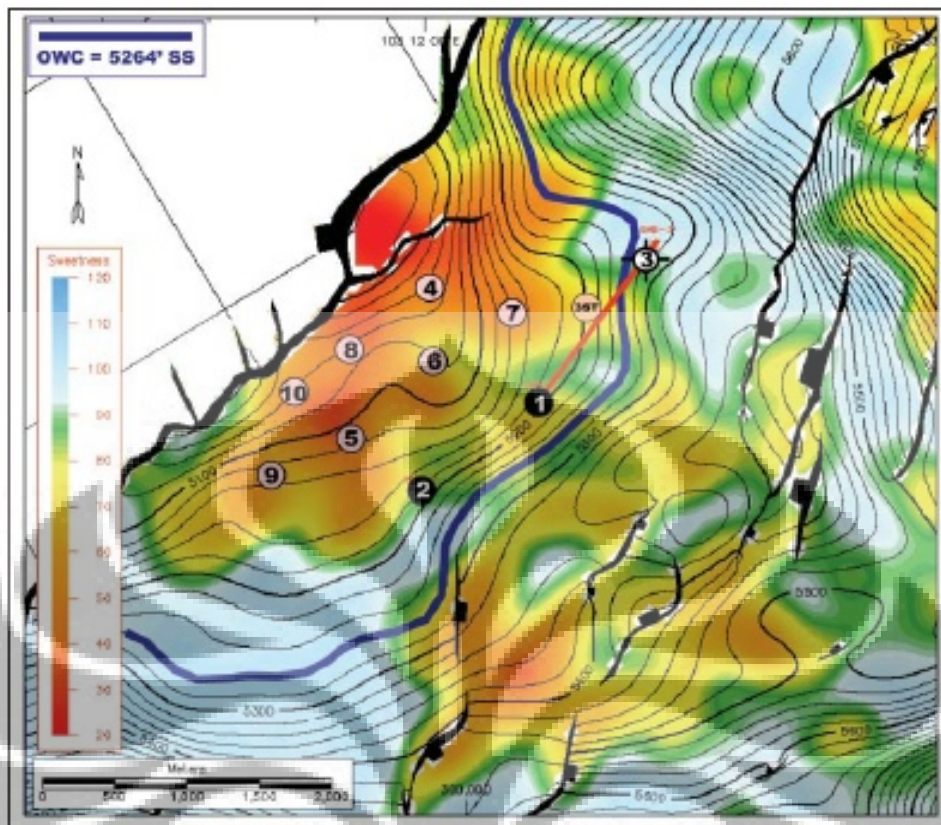


Figure 3.4 Horizon slice from top A-Sand showing sweetness overlain on the depth contour structure map. The pink circles represent eight new development wells. The blue contour line represents the oil-water contact. The correlation between low values of sweetness and high porosity

### 3.2.2 AVO

AVO is a useful tool to help understand the rock and fluid properties of the earth. It has proven itself useful for finding hydrocarbons. Interpretation based on an AVO analysis provides more information than an interpretation based just on conventional stacked seismic. The stack, used in a conventional interpretation, represents the average amplitude found in the multi-offset data at a particular location. It is an approximation of the bandpassed P-wave impedance reflectivity, where P-impedance is the product of P-wave velocity and density, and the reflectivity is the difference of the P-impedance divided by its sum at each geological layer boundary.

In AVO analysis, instead of just looking at the average amplitude, the amplitudes of all the offsets are analyzed. It is possible to summarize the AVO behavior with several parameters that can be output as sections. These sections can be related to the reflectivity of various elastic parameters. For example, after AVO analysis it is possible to generate both the bandpassed P-wave and S-wave impedance reflectivity, where S-wave impedance is the product of S-wave velocity and density. So, instead of just interpreting an approximate form of the P-impedance reflectivity stack as in a conventional interpretation, both the P and S impedance stacks can be interpreted in an AVO analysis allowing the interpreter to more uniquely describe their geologic objective. This is the promise of AVO. A number of considerations temper the reality.

First the relationship between the rock properties and the elastic parameters is non-unique. The elastic parameters are what we can measure with the seismic. There are at most three parameters: P-wave velocity, S-wave velocity, and density. However, there are many rock and fluid variables that influence the elastic parameters. Hence, any predictions made about the rock properties from elastic parameters will be ambiguous.

Secondly, the elastic parameters are not measured directly. Elastic waves are measured which have propagated through the earth. These waves are distorted and must be properly processed in order to get useable estimates of the earth's elastic parameters. If this is not done correctly, there will be errors in the elastic parameter estimates and the subsequent geologic prediction. In fact, it is virtually impossible to recover the true elastic parameters of the earth from seismic measurements due to three fundamental limitations in the seismic method: the effect of the bandpassed seismic wavelet, the distortion of the seismic raypath due to unknown geologic structure and velocity, and the effect of seismic noise.

Many AVO approaches make extensive use of models. But how well can we model seismic data? If we accept models of the seismic reflection process that incorporate separated sources and receivers, then we must, by implication, believe that we can model with coincident sources and receivers (Hampson, D, 1991). This would certainly hold true in a one-dimensional case (e.g., the synthetic

seismogram calculation). It is now well established that the widely used Gassmann equation (1951) understates the effect that replacing water with oil or gas as the pore fluid has on seismic velocity.

Based on what we do know from the physics of models amplitude levels at increasing offset will be reduced algebraically when oil or gas replace water as the pore fluid, under a wide variety of common circumstances, and irrespective of the rock matrix character or condition. The effect is generally more pronounced in young, unconsolidated rocks, and for gas, light oil or high gas-oil ratios (GOR), rather than for oil alone. Of course, this conclusion requires little in the way of quantitative specifications. But alternate approaches to AVO that demand precise specification of quantities (e.g., shear wave velocity or Poisson's ratio) may be making unrealistic demands on the present state of technology, for reasons which are still not generally appreciated. Burnett (1990) documents a typical case of the success of AVO methodology, yet accompanied by a puzzling but dramatic failure of AVO models.

### **3.2.2.1 AVO Attributes and Techniques**

Many different AVO attributes that could be compared and contrasted, there are six different methods that usually applied to doing AVO analysis. Three methods are combinations of intercept and gradient computations or equivalent measurements. These three uncalibrated attributes are scaled Poisson's ratio change, far-minus-near times far, and Smith and Gidlow's fluid factor. Two inversion AVO attributes (attributes generated by inverting the basic AVO attributes, combinations of these attributes, or offset substacks) elastic impedance and the  $\lambda\rho/\mu\rho$  ratio—are also examined (Castagna, 2000). The final AVO attribute considered is a calibrated neural network AVO (NNAVO) created by training a neural network to approximate time-based well control using the AVO intercept, gradient, and migrated stack.

Perhaps the most widely publicized practical use of AVO applications is gas detection. Both Backus et al. (1982) and Ostrander (1984) provide a good

basis for discussing this topic (Castagna, 1997). Both studies make extensive use of seismic models, although the Backus work is more theoretical and does not indicate field results. Backus and his colleagues, however, use their model studies to provide still further reasons as to why we should not always expect good correlation between log-derived synthetic results and field seismic data particularly for certain geologic provinces, and certainly not without appropriate considerations for the seismic data.

One of Ostrander's models (Figure 3.5) represents a thick gas-filled sand. Sand unit thickness is important in determining offset behavior. In this case, specific sands are being modeled, and we will view field data with an eye toward this model. Figure 3.6 shows field data that contrasts amplitude with offset variation for gas-filled sands and sands without gas.

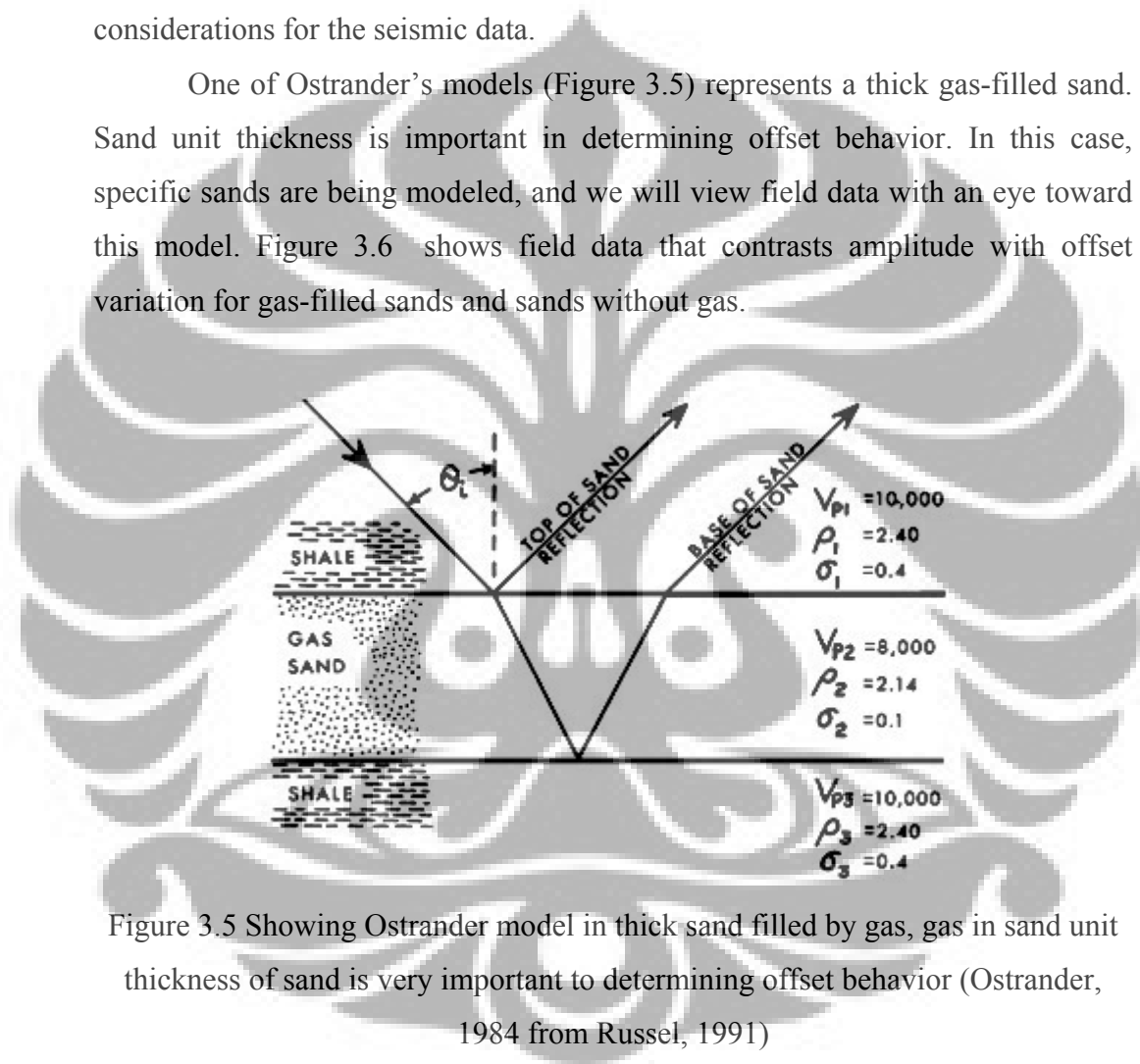


Figure 3.5 Showing Ostrander model in thick sand filled by gas, gas in sand unit thickness of sand is very important to determining offset behavior (Ostrander, 1984 from Russel, 1991)

To improve signal-to-noise conditions, ten adjacent moveout-corrected and summed CDP gathers representing the two cases are noted. Near offsets are depicted to the right in each gather.

In Figure 3.6 the gas-filled zones encompass shot points 80, 81, 101 and 102. Each case, whether noted in the CDP gather single-fold or with a 10-fold vertical sum, shows substantial amplitude increase with offset. Shot points 140, 141, 142 (and where gas is not present) show no comparable effect.

Two basic conclusions from Ostrander's work are poisson's ratio has a strong influence on changes in reflection coefficient as a function of angle of incidence and analysis of seismic reflection amplitude versus shot-to-group offset can, in many cases, distinguish between gas-related amplitude anomalies and other types of amplitude anomalies. Numerous such analyses have been performed on seismic data recorded over known gas sands. Additionally, there have been analyses performed on seismic bright spots recorded over high velocity volcanics, basalts, and conglomerates. Results have often been encouraging, reducing exploration risks on prospects showing apparent seismic bright spots. Some failures have occurred, however, usually in provinces of higher velocities and densities where the lithology is more consolidated.

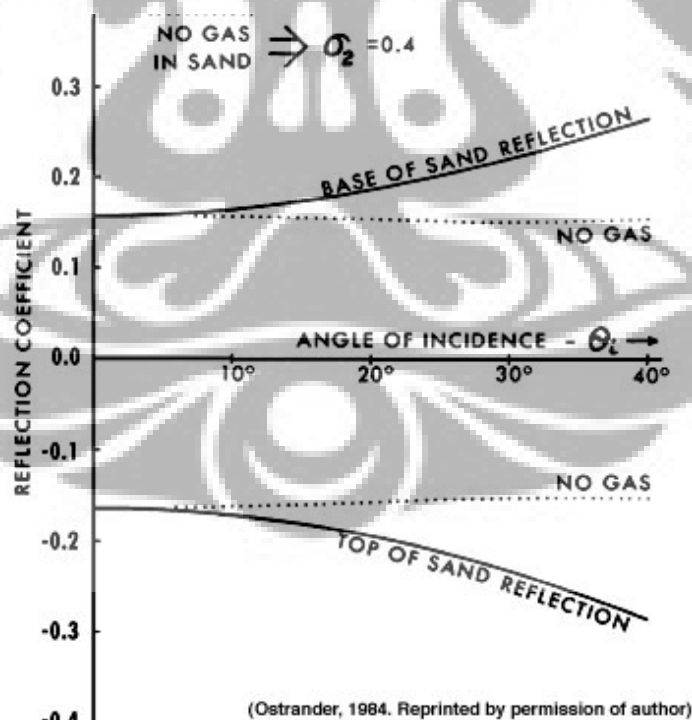


Figure 3.6 Showing Ostrander model in field data that contrasts amplitude with offset variation for gas-filled sands and sands without gas

Long (1985) offered an innovative color display of amplitude variation with offset. The colors represent the slopes of the amplitude with offset variation, with red indicating the greatest increases with offset. Of course, the interpretive process needed to confirm and understand the origin of the anomalies would have to follow from the previous discussions. It is always true that AVO anomalies cannot be interpreted in terms of their lithologic significance without some appreciation of the geologic setting and expressed in terms of acoustic parameters. It is clear also that modeling technology and calibration work are necessary tools for obtaining the maximum amount of information.

### 3.2.2.2 Aki and Richard (1980)

Zeopritz (1953) derived a relationship governing the reflection and transmission coefficients for plane waves as a function of angle of incidence and six independent elastic parameters, three on each side of the reflecting interface. These three elastic parameters are  $V_p$ ,  $V_s$  and density. This problem was further investigated by Koefoed (1955), who calculated by hand the reflection coefficient versus angle of incidence up to  $30^\circ$  for 17 different sets of elastic properties. He computed the reflection coefficient using the three elastic parameters  $V_p$ ,  $\rho$  and  $\sigma$ ; his method was laborious (From Russel, 1993).

Recently the dependence of seismic reflection amplitude upon offset between source and receiver has been thoroughly investigated by Ostrander (1984), Searwood et al (1983), Gassaway and Richgels (1983), Shuey (1985), and Hilterman (1986). Shuey (1985) proposed a simplification of the Zeopritz equations that will be presented in this discussion, as it is widely used to compute Poission's ratio as a function of reflection amplitude and angle of incidence. Hilterman (1986) modified Shuey,s equation and established a linear equation governing the relationship between incident angle and reflection coefficient.

Aki and Richard simplification the Zoeppritz equation to the following:

$$R(\theta) = a \frac{\Delta V_p}{V_p} + b \frac{\Delta \rho}{\rho} + c \frac{\Delta V_s}{V_s}$$

University of Indonesia

dengan :

$$a = \frac{1}{2 \cos^2 \theta},$$

$$b = 0.5 - \left[ 2 \left( \frac{V_S}{V_P} \right)^2 \sin^2 \theta \right],$$

$$c = -4 \left( \frac{V_S}{V_P} \right)^2 \sin^2 \theta,$$

$$\rho = \frac{\rho_2 + \rho_1}{2}, \Delta\rho = \rho_2 - \rho_1,$$

$$V_P = \frac{V_{P2} + V_{P1}}{2}, \Delta V_P = V_{P2} - V_{P1},$$

$$V_S = \frac{V_{S2} + V_{S1}}{2}, \Delta V_S = V_{S2} - V_{S1},$$

$$\text{and } \theta = \frac{\theta_i + \theta_t}{2}.$$

The first term, A, is a linearized version of the zero offset reflection coefficient and is thus a function of only density and P-wave velocity. The second term, B, is a gradient multiplied by  $\sin^2\theta$ , and has the biggest effect on amplitude change as a function of offset. It is dependent on changes in P-wave velocity, S-wave velocity, and density. The third term, C, is called the curvature term and is dependent on changes in P-wave velocity only. It is multiplied by  $\tan^2\theta \cdot \sin^2\theta$  and thus contributes very little to the amplitude effects below angles of 30 degrees.

### 3.2.2.3 AVO Classification by Rutherford and Williams

Hydrocarbon related “AVO anomalies” may show increasing or decreasing amplitude variation with offset. Conversely, brine-saturated “background” rocks may show increasing or decreasing AVO. Amplitude - versus - offset interpretation is facilitated by crossplotting AVO intercept (A) and gradient (B). Under a variety of reasonable geologic circumstances, As and Bs for brine-saturated sandstones and shales follow a well-defined “background” trend. “AVO anomalies” are properly viewed as deviations from this background and may be related to hydrocarbons or lithologic factors.

The common three-category classification developed by Rutherford and Williams and have be revised by Castagna with add Class IV category should be considered (Figure 3.7). Superimposed an example of a Class IV gas sand on a



figure taken from Rutherford and Williams which shows their gas-sand classification based on normal incidence reflection coefficient. The vertical axis is reflection coefficient and the horizontal axis is local angle of incidence. Note that Class III and IV gas sands may have identical normal incidence reflection coefficients, but the magnitude of Class IV sand reflection coefficients decreases with increasing angle of incidence while Class III reflection coefficient magnitudes increase. These are low impedance gas sands for which reflection coefficients decrease with increasing offset; they may occur, for example, when the shear-wave velocity in the gas sand is lower than in the overlying shale. Thus, many “classical” bright spots exhibit decreasing AVO. If interpreted incorrectly, AVO analysis will often yield “false negatives” for Class IV sands. Clearly, the conventional association of the term “AVO anomaly” with an amplitude increase with offset is inappropriate in many instances and has led to much abuse of the AVO method in practice. Similarly, interpretation of partial stacks is not as simple as looking for relatively strong amplitudes at far offsets.

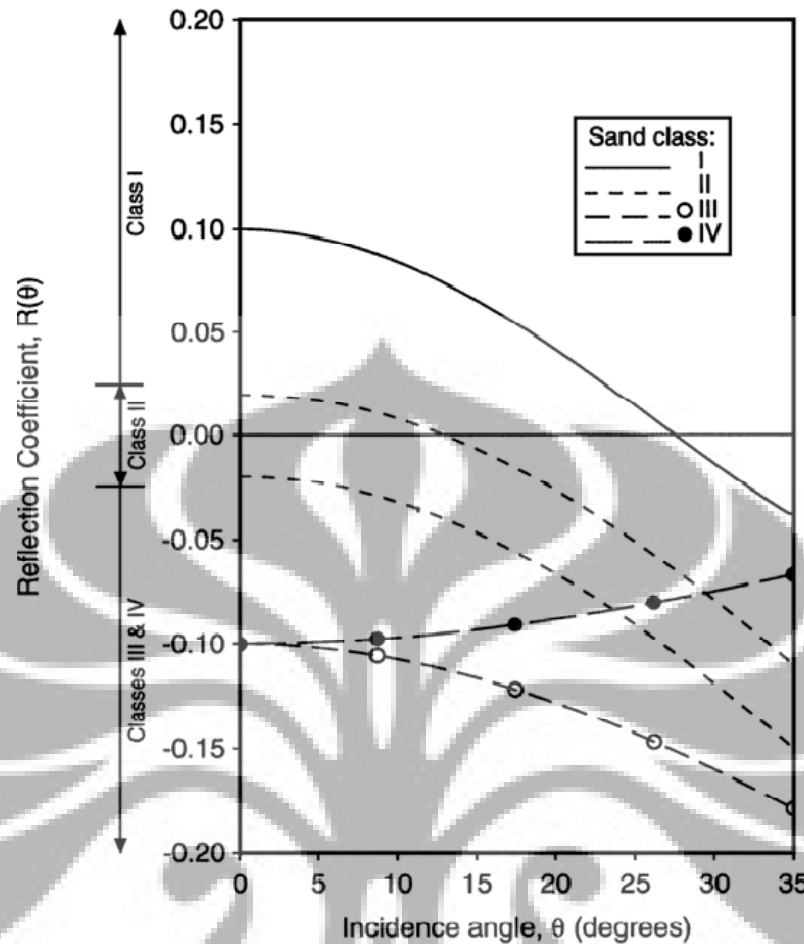


Figure 3.7 Superimposed an example of a Class IV gas sand on a figure taken from Rutherford and Williams which shows their gas-sand classification based on normal incidence reflection coefficient (Castagna et al., 1998)

#### 3.2.2.4 Bright Spot and Dim Spot

AVO behavior as a means of classifying reservoir rocks presents in itself some serious ambiguities. Because AVO effects at a reservoir boundary involve both the reservoir and the host rock (usually overlying), implicit assumptions may not always be valid. For instance, Rutherford and Williams (1989) proposed a classification of sand reservoirs based on AVO response character, assuming that the host rock is normally pressured shale. While this assumption may work for much of the Gulf of Mexico, it is often inapplicable in a global context.

As with the classification of seismic reflectivity and amplitude responses (i.e., zonation), an AVO classification, or category, has been proposed. We can note commonly occurring cases of sands like the Wilcox in Grant Co., Oklahoma, U.S. (Landwer, Neidell and Smith, 1992) or the Rotliogendes of the North Sea (Ahmed, 1991). According to Rutherford and Williams, these should be Category I sands; instead, they exhibit Category II and III AVO signatures, since they are overlain, respectively, by a carbonate and an evaporite. Also, we can readily see how a Category III AVO responsive sand (based on Rutherford and Williams' scheme) can demonstrate Category I character if the encapsulating shales are overpressured.

Analogously, the carbonate porosity developed in the Swan Hills of the Caroline Field, Alberta, Canada (Morris and MacGregor, 1992) is noted as a pronounced trough, since the overlying shale is an argillaceous limestone. The AVO signature is much like a Category III sand rather than what we might expect for a carbonate. In fact, the same unit of carbonate porosity under a shale could be characterized by either a peak or a trough, depending on whether or not it forms the carbonate unit upper boundary. The AVO signatures of the corresponding seismic event would then be quite different (Figure 3.8).

The preferred method is to base sand reservoir classification on sand/shale reflectivity character. As a standard, we compare water-wet sand to normally pressured, contemporary aged shales. In Zone I, the sands are consistently low in their velocity-density product (acoustic impedance) compared to normally pressured contemporary aged shales—the "bright spot" regime. In Zone III, the sands are consistently higher than the shales in acoustic impedance, because the sands have consolidated in crossing through the shale level. Zone II is the crossover regime for sand/shale reflectivity, having a large population of sands which are quite anomalous in their seismic response with regard to porosity and fluid content. These are largely responsible for the traditionally poor fits with sonic and density log-based synthetic seismogram calculations.

Neidell and Berry (1989) introduced many of the ideas expressed above. Advantages of this scheme over an AVO-based approach include, among other

benefits, applicability over a much broader range of sandstone depositional environments.

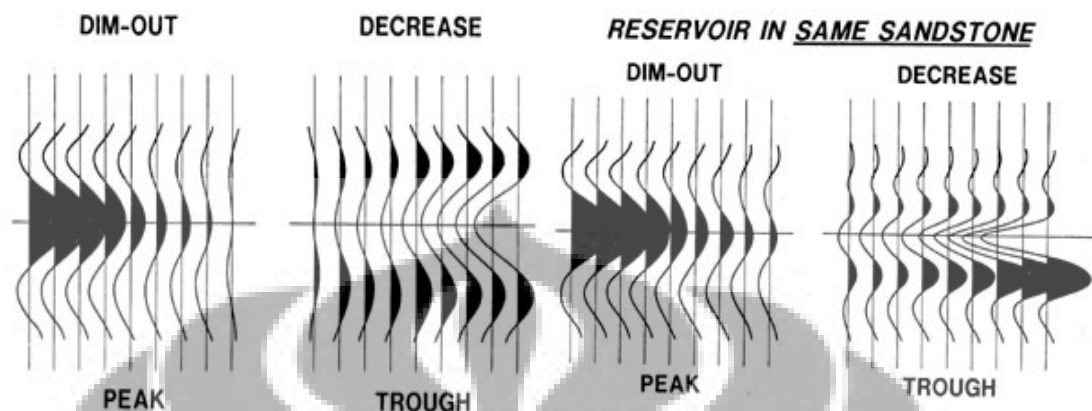


Figure 3.8 The AVO signatures of the corresponding seismic event would then be quite different

### 3.2.2.1 Limitations of the AVO Method

Like other stratigraphic modeling techniques, the AVO method has several limitations. Recently, a few published papers, such as Hilterman (1990) and Swan (1991), have documented case studies citing failures of AVO. The authors have also postulated the reasons why the method failed.

One of the most obvious reasons why the modeled data may not match the real data is waveform stretch. We noted earlier in the text that NMO corrections artificially stretch seismic waveforms. Waveform stretching also occurs in the migration process. Although stretching is not a major factor, its greatest effect occurs when we correct for moveout in low-velocity mediums. Thus, where we tend to use AVO the most frequently—in low-velocity gas sands—the risk of amplitude stretch is the greatest. One way to minimize these effects is to use un-NMO corrected and unmigrated CDP gathers. We must also realize that AVO models are highly susceptible to small changes in the input parameters, in particular Poisson's ratio. And unfortunately, Poisson's ratio is one of the parameters we know the least about. A third cause for concern is the Domenico effect—a small amount of gas has almost the same effect on amplitude as does a

large amount of gas. Therefore, when we see an increase or decrease in amplitude due to the presence of gas, we generally cannot predict the quantity of gas present.

Another limitation to the method is homogeneity of the model, both laterally and vertically, versus the inhomogeneity of the subsurface. We naturally would like every relationship between an AVO response and a rock property to be linear and unique, but this is not often the case. In a study by Hiltebert (1990) of the Ship Shoal-South Addition area in the Gulf of Mexico, one of the reasons for the failure of the AVO method was that the existence of five different shale types in the study area went unrecognized. Thus, using a single velocity versus density trend for the shales in the model did not reflect the true complexity of the area. Another reason for failure cited by Hiltebert was that the "AVO response for a sand package depends not only on the degree of shaliness but also the shale distribution within the sand package." This inhomogeneity was also not considered in the model.

And of course, we must always be aware of possible amplitude tuning effects. Figure 3.9 shows a wedge model in which amplitude tuning occurs. Also shown in the figure are selected relative amplitude common midpoint (CMP) gathers. In these gathers we see an increase of amplitude with offset which is due not to the presence of gas, but to tuning effects. And finally, AVO solutions, like all stratigraphic modeling solutions are non-unique. Although our modeled solution may match our observed data, there may be another set of model parameters that could generate the same synthetic seismic response. For example, as we see in Figure 3.10, highly porous water-wet sandstones can cause an increase in amplitude with offset similar to that caused by gas sands with lower porosity.

In summary, AVO modeling can play a valid role in the prediction of subsurface stratigraphy. But, we must completely understand the nature of the geologic input parameters and their impact on the seismic response. We must also understand that when we compare AVO models to the real data, the obvious solution is certainly not a unique one, and may not be the correct one. We should use other modeling techniques to support our interpretation.

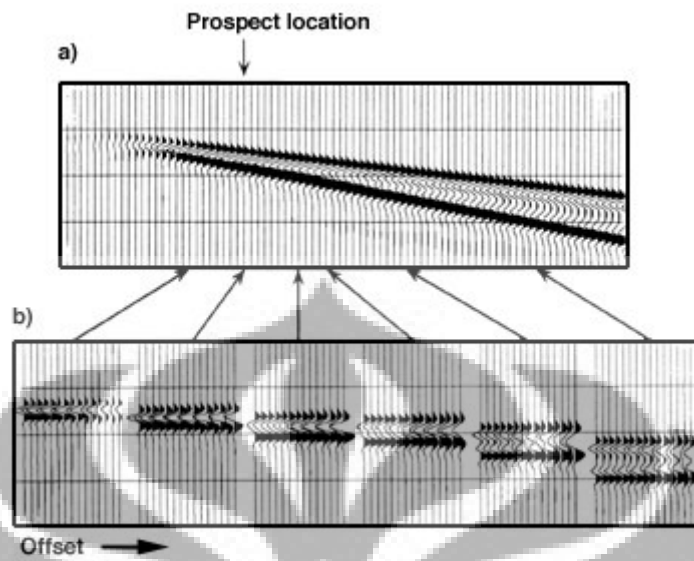


Figure 3.9 Wedge model in which amplitude tuning occurs (Allen and Peddy, 1993)

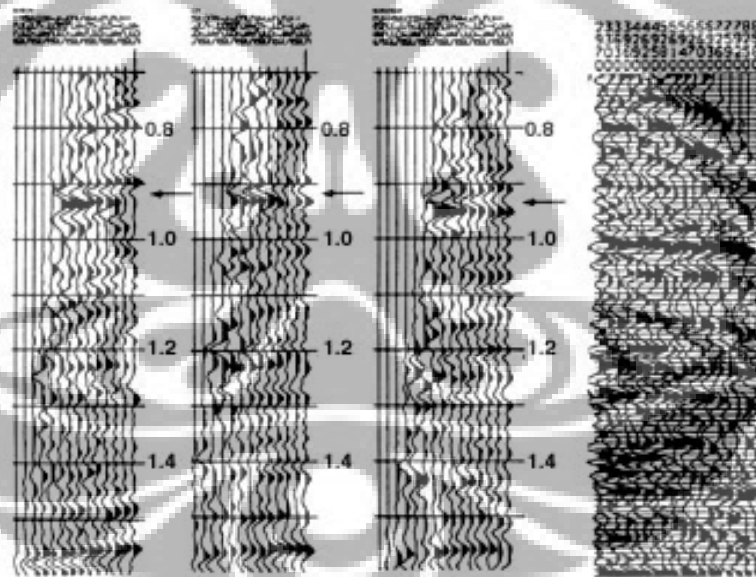


Figure 3.10 Highly porous water-wet sandstones can cause an increase in amplitude with offset similar to that caused by gas sands with lower porosity (Allen and Peddy, 1993)

## Chapter 4

### Result and Discussion

#### 4.1 Data Preparation

##### 4.1.1 Well Conditioning

Well conditioning was needed in Cantik field. After log check in every well, there was some problem. Almost in every wells density and sonic log was not calibrated with caliper. In the first step, we need calibrated with all log data. Example of log editing based in calibration from caliper, GR and SP can see in well F-4 (Figure 4.1).

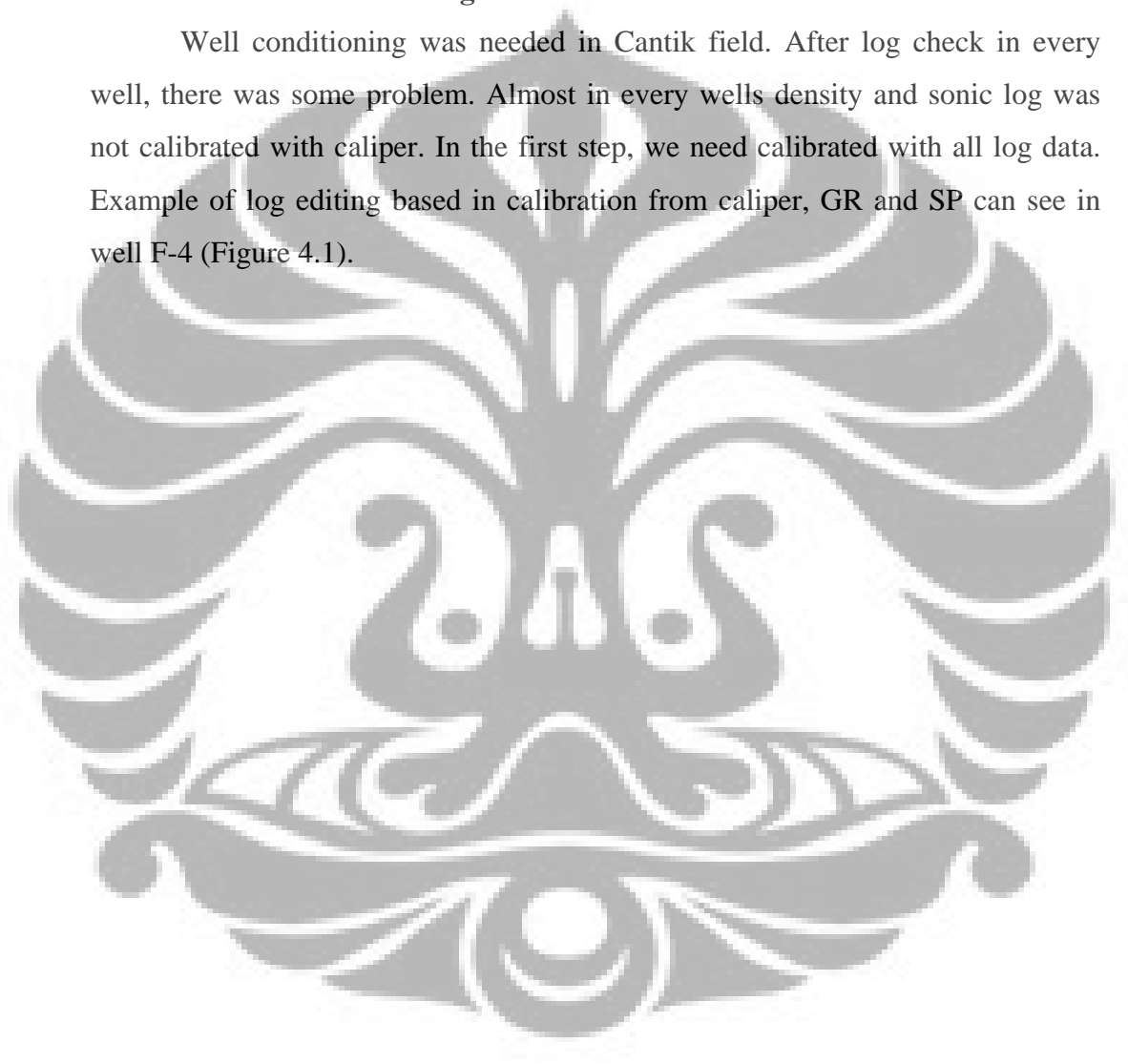


Figure 4.1 Well conditioning in F-4, showing log editing in density log and sonic log base on caliper, GR and SP analysis

Density log and Sonic log edited by give a straight line with the same value at top of log. Usually at the top of log the logging tools were not running. So there was a gap of log data. In well seismic tie usually the bad correlation

between seismic and well happen because the missing data at the top of logging tools. We need to reduce the shifting and stretching seismic.

Another important thing was borehole problem. In areas that have a borehole problem, just like loss circulation give the wrong log data. To show the relationship between the borehole data problem can be look from the caliper data. In areas that have a high caliper value was areas that have a wrong logging result. In those areas we were doing some editing. After editing in areas that have borehole problem, we also doing the smoothing. Smoothing was done because we want erased spiking data.

#### **4.1.2 Well Seismic Tie**

Well seismic tie in Cantik field was done in all wells. Cantik field have 2 wells with checkshot data. For the deviated wells in Cantik field does not have a checkshot data. Checkshot data is located in F-1 and F-2. Checkshot in F-1 was not having problem, but the problem was happened in F-2. When the velocity was calculated in F-2, in some zones the velocity data are negative (Figure 4.2). Because of that result, before we can use the checkshot data, we must do some editing zone.

Editing zone data was done with erased TWT and Depth data in F-2 checkshot that have negative velocity value (Table that show the checkshot editing was in attachments in Table 1 and 2). After the editing result we doing the recalculated velocity and doing the crossplot between velocity and depth, to see the relationship of checksoot result. From figure 4.2 checkshot data in F-2 was ready to use.

The next step when we doing the well seismic tie defined the wavelet. Wavelet extraction is doing in every well. Example in F-1, frequency dominant in F-1 is 5-70 Hz, in maximum frequency is in 30 Hz. With the frequency calculation, possibility of vertical resolution in Cantik field area was about 50-60 feet.



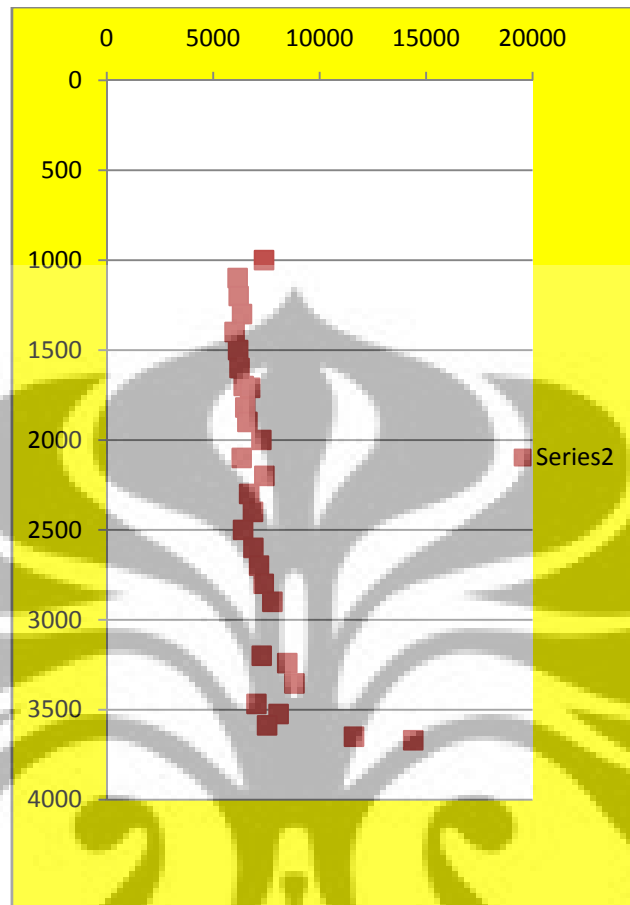


Figure 4.2 showing crossplot result from depth and velocity data in F-2

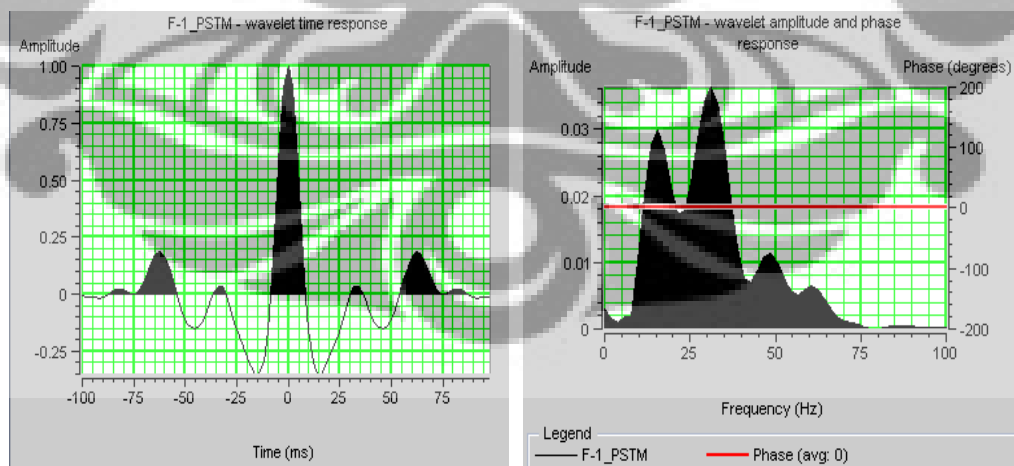


Figure 4.3 showing wave extraction in well F-1, with parameter wavelet length 200 ms; taper length 25 ms and sample rate 2 ms

From the well seismic tie in F-1, the correlation value was 0,84 (Figure 4.4). The result is very good, and for another well, the correlation range is in between 0.45-0.85. From that correlation value, the result of the well seismic tie in Cantik field is good and ready to used.

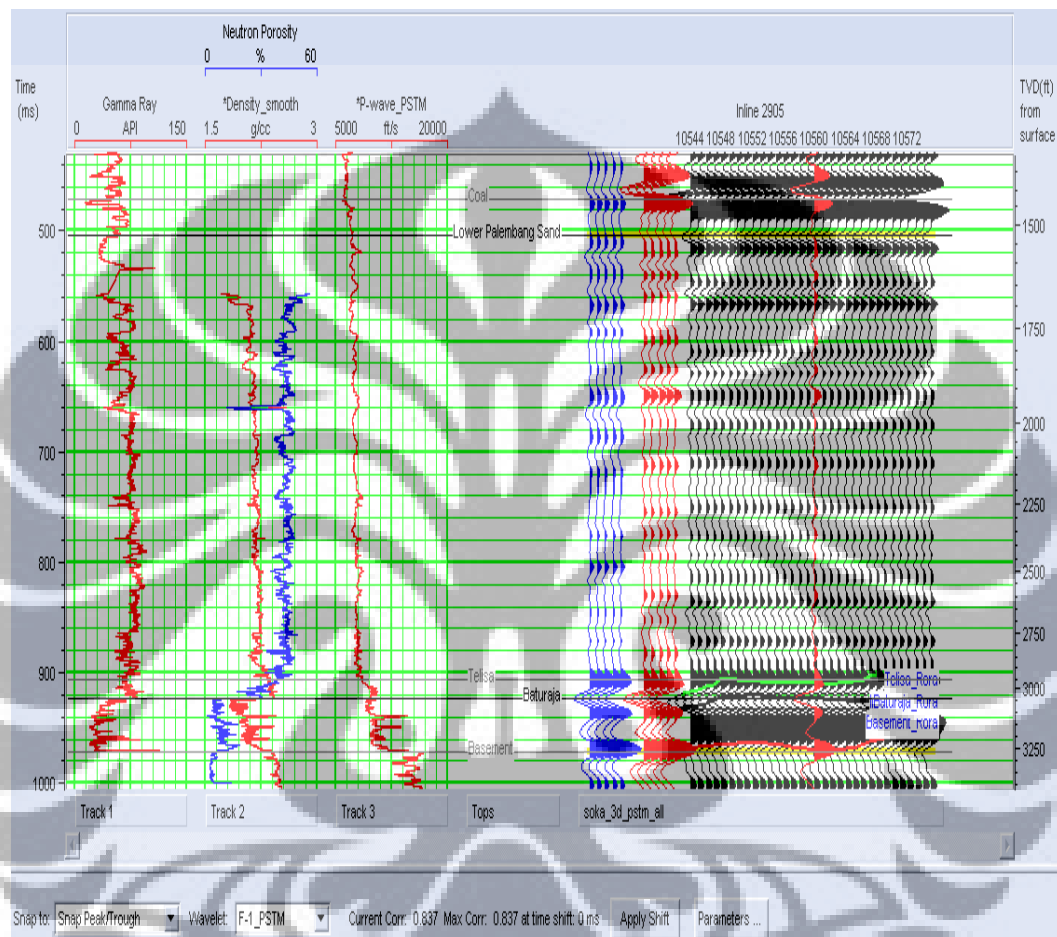


Figure 4.4 Showing well seismic tie result in F-1, using wavelet F-1\_PSTM, showing the 0.84 correlation result

From well seismic tie result and seismic phase calculation in every seismic section of wells area, there was some unusual result. From phase calculation in Cantik field in wells F-1, F-8 and F-11 the calculation of phase is rotate with range  $145^{\circ}$ - $180^{\circ}$  (Figure 4.5), but result of another wells is not significant rotate (Figure 4.6). With that result assumed that seismic in Cantik field area mix phase with the major phase is normal phase.

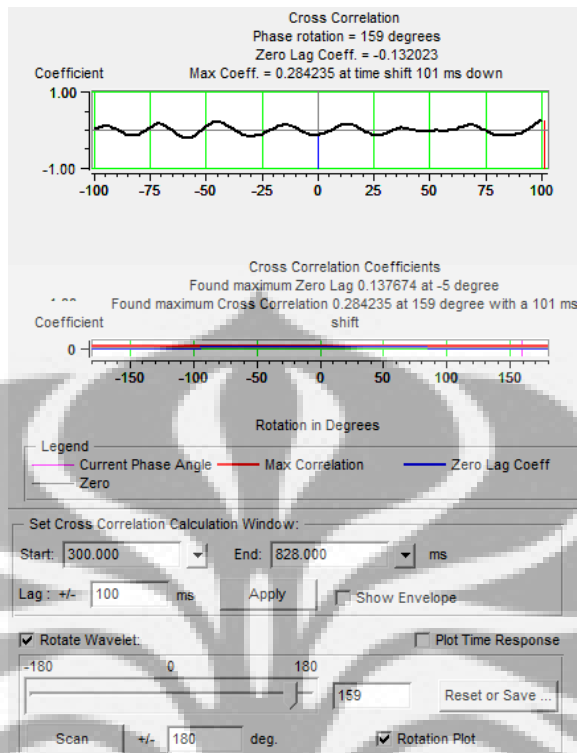


Figure 4.5 Showing 159° rotation phase in well F-1 makes the polarity in F-1 was reversed polarity.

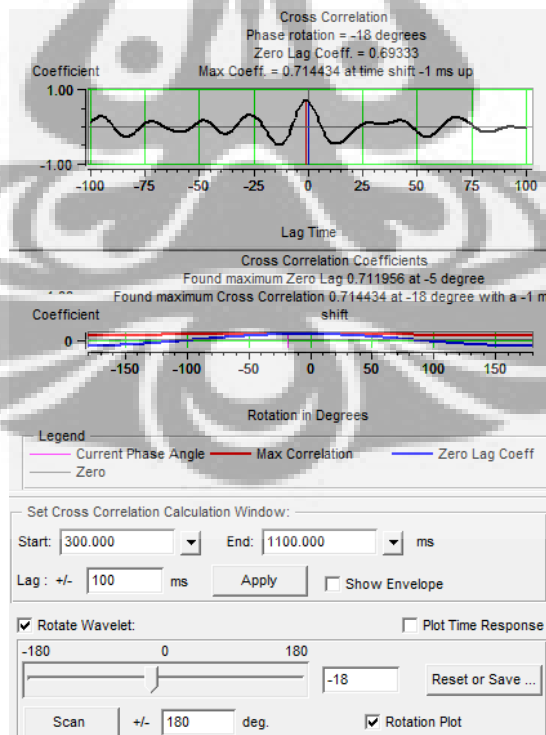


Figure 4.6 Showing -18° rotation phase in well F-5 makes the polarity in F-1 was normal polarity

### 4.1.3 Seismic Interpretation

After well seismic tie in 16 wells in Cantik field, we start seismic interpretation. From the well seismic tie result there was some unusual result. After we try to correlate between well to well, the top of Baturaja was not consistence. In area that filled by gas baturaja is consistence in trough but in area that filled by oil is consistence in pick (Figure 4.7). From this result make guidance that horizon interpretation in Cantik field is guide by fluid filled. But the result was still need to prove by fluid substitution analysis, to see the sensitivity of fluid content in seismic section.

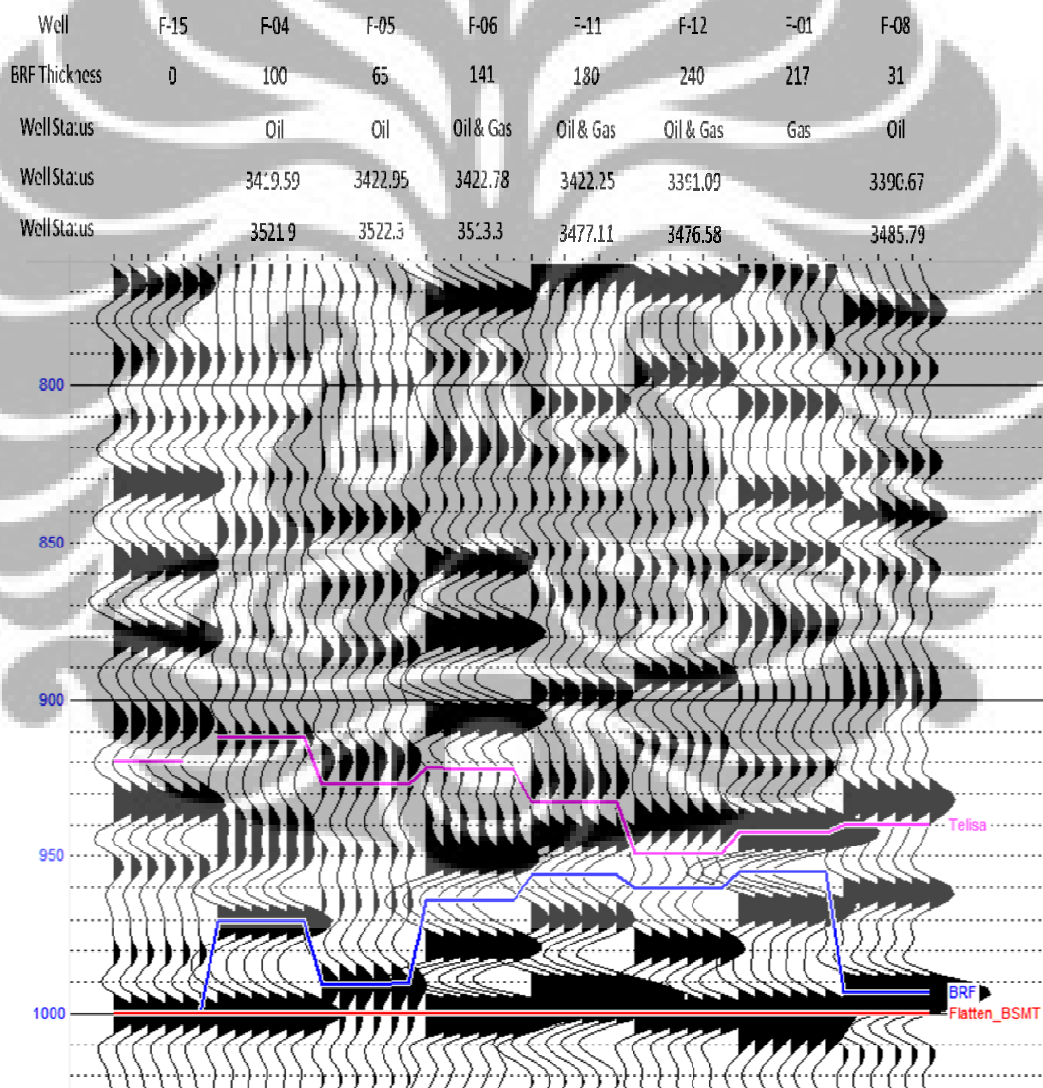


Figure 4.7 Seismic section in wells location that showed seismic interpretation in Baturaja was depending by fluid content

But from the well seismic tie is not enough, we need some quantitative model to see the reflection coefficient in well that have already fill by 100% oil and 100% gas. I was doing calculation in 2 key well, for well that have 100% gas was represented by F-1 and well that represented by 100% oil was in F-4. From the RC calculation in those 2 wells, we can see the differences of RC value. In F-1 the RC calculations was about -0.0048, and in F-4 the RC calculations was 0.001484 (Complete calculation in Table 3 and 4 (attachements)). With that evidence we can see well seismic tie result was correct, seismic data in this area was depends by fluid content.

Another interesting thing that we can see in that figure was the relationship of tuning effect. In well F-5 and F-8, thickness of Baturaja was thin. The thickness was range by 30 – 50 feet. From F-5 and F-8 case, Baturaja was filled by oil and made seismic interpretation in Baturaja was in peak. But for the basement, because baturaja thickness was under of tuning effect basement is in near of zero crossing. That case made a new concept seismic interpretation of Baturaja distribution change. Distribution of oil in Cantik field is in flank area. We have difficulties to identify distribution of Baturaja in Flank area. With that concept makes various of interpretation about baturaja in flank area, just like in crossline 10600 (Figure 4.8).

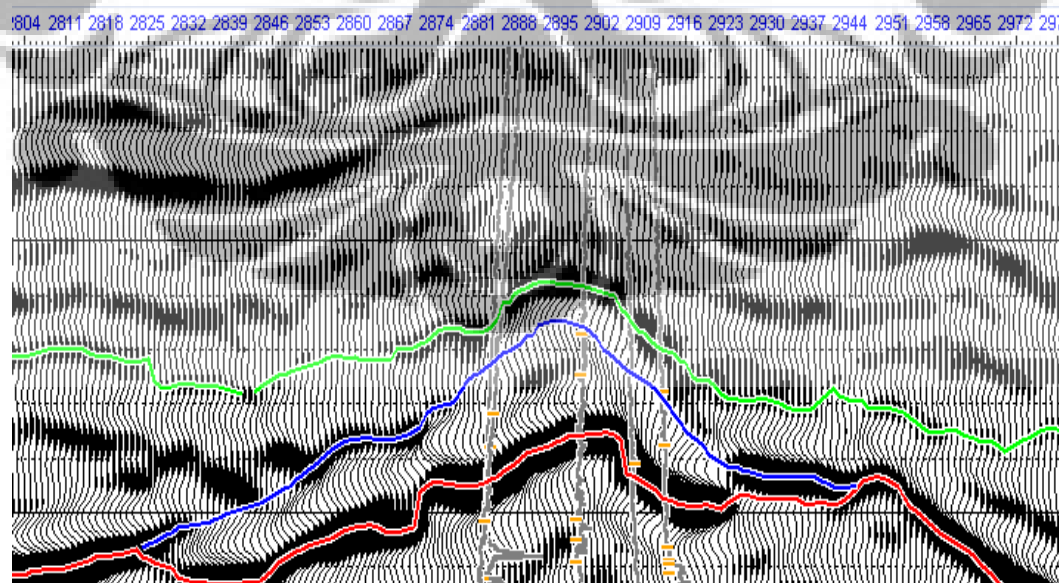


Figure 4.8 Show interpretation of Baturaja formation that possible because tuning effect

In generally Baturaja identification was difficult, especially in flank area. So we need to doing looping interpretation, so can define Baturaja distribution in every area in Cantik Field (Figure 4.9).

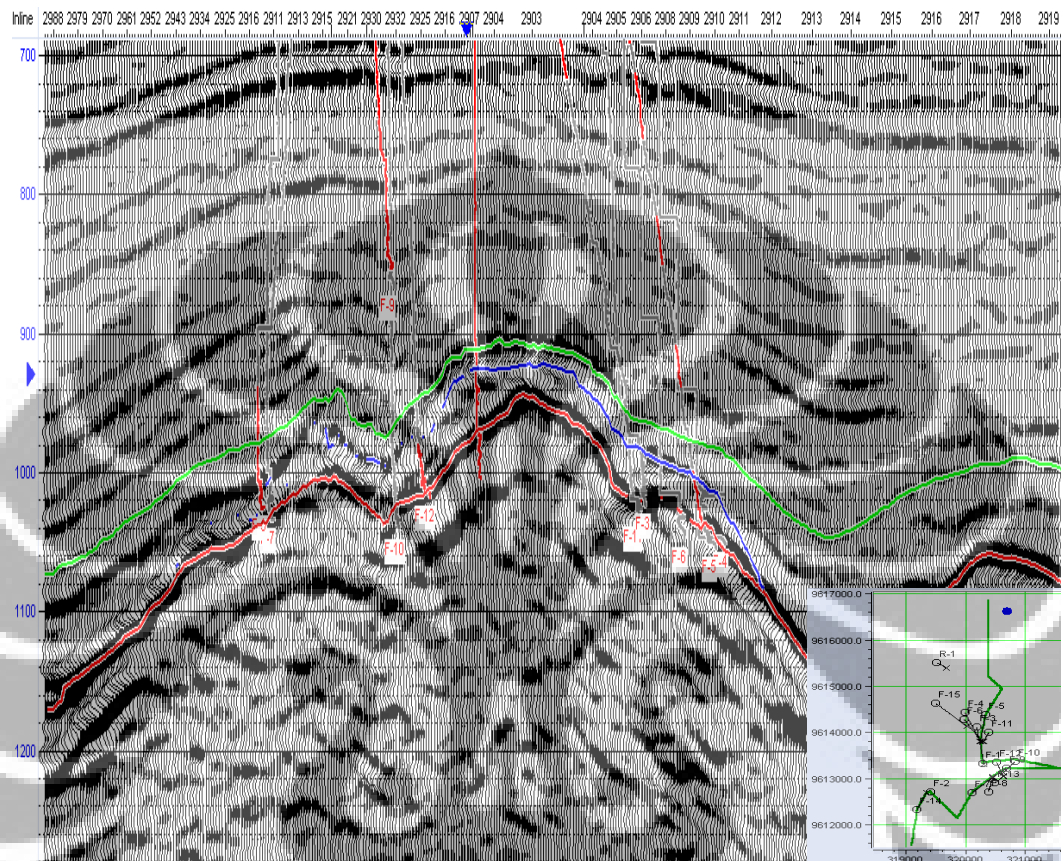


Figure 4.8 Show seismic interpretation trespassing wells in Cantik field

## 4.2 Result of Fluid Substitution

According to Gassmann's equation, the fluid substitution effect is a result of the interplay between the mineral module, the dry frame module, fluid bulk modulus and porosity. We introduce a model which allows the dry frame module to be determined in terms of the mineral module, porosity and a geometry factor, which we denote by the letter  $a$ .

Fluid substitution was doing in two wells. F-11 and F-12 have shear wave data. From fluid substitution study need initial data of formation (Figure 4.9). Initial data was needed were pressure, gas gravity, temperature, oil gravity, gas-oil ratio and salinity.

From well test report in F-12 we can find that pressure in Baturaja zone is about 2900 PSI. Oil gravity value was 0.6. Initial temperature while drilling was 80 degree. For oil gravity of Baturaja was 30 API. Gas Oil ratio of Baturaja formation was 100 L/L. And the salinity was 10000 ppm. The salinity was only prediction, because in that well was not have salinity test result.

**Set Parameters for Fluid Properties Calculations**  
This menu calculates the density and bulk modulus of the fluids

Pressure: Constant = 2900.653 PSI

Gas Gravity: Constant = 0.600

Temperature: Constant = 80.000 Degrees C

Oil Gravity: Constant = 30.000 API

Gas-Oil Ratio: Constant = 100.000 L / L

Salinity: Constant = 10000.000 ppm

---

**Results of Fluid Properties Calculations** Sample # 0 4128.14 m.

	Oil	Gas	Brine	Pore Fluid	
Calculated Density:	0.7367	0.1295	0.9885	0.7367	(g/cc)
Calculated Modulus:	0.2925	0.0405	2.5385	0.2925	(GPa)
Saturation:	1.00	0.00	0.00		[frac]
Saturation GOR:	88.549				(L/L)
Water Flash Pressure:	0.0406				(MPa)

Calculate

Figure 4.9 Show fluid substitution properties calculation window in well F-12

Result of fluid substitution in F-11 and F-12 showed that seismic section in Cantik location was influenced by fluid content (Figure 4.10). From picture below, the black seismic wiggle is original Pre stack Time Migration in F-12 well. When log data substituted by 100% gas top of Baturaja not changed, still in trough part. But when the log data substituted by 100% wet top of Baturaja changed become peak. From this result make higher confidence level that seismic interpretation base on well seismic tie before was already corrected. The P-wave depends only very weakly on the fluid saturation on account of the high mineral

bulk modulus; this is not disturbed by a dynamic fluid substitution effect. Similarly, the fast shear wave behaves according to the Gassmann equation. The only real deviation from Gassmann occurs for the slow shear wave. This can be strongly influenced by the concept of dynamic fluid substitution. We are therefore led to the somewhat surprising conclusion that shear-wave splitting is potentially the attribute which is most sensitive to the saturating fluid in carbonate rocks.

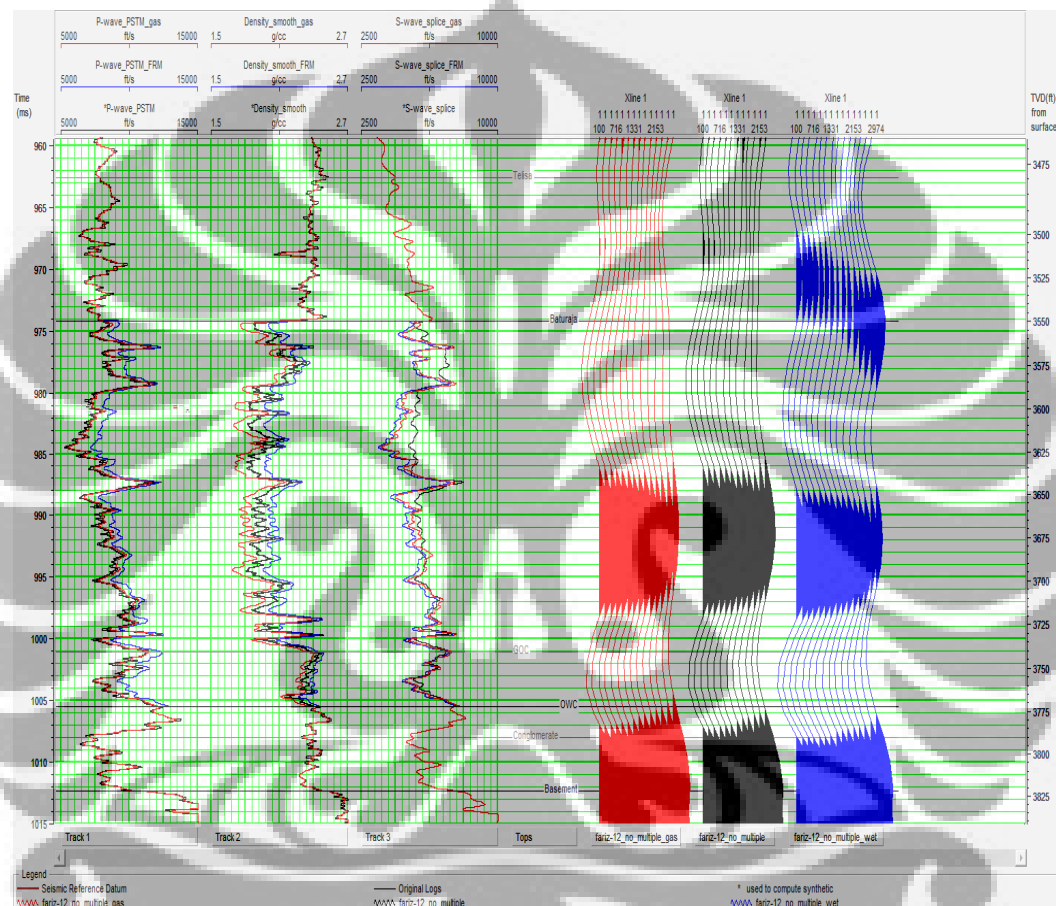


Figure 4.10 Show fluid substitution result in well F-12, the black wiggle showed original seismic data, red wiggle showed fluid result substitution replace by 100% gas and blue wiggle showed fluid substitution result replace by 100% wet

### 4.3 Result of Sweetness Attribute

To further evaluate their internal properties, particularly to infer these geobodies reservoir potential, another derivative volume namely “sweetness” was created. This volume is basically a ratio between instantaneous amplitude (Figure 4.11) over square root of the instantaneous frequency (Figure 4.12).



Figure 4.11 Result Amplitude envelope in line 2905, Cantik field area, South Sumatra Basin

Instantaneous frequencies relate the wave propagation and depositional environment, hence they are physical attributes and they can be used as effective discriminators:

- Corresponds to the average frequency (centroid) of the power spectrum of the seismic wavelet.
- Seismic character correlator in lateral direction,
- Indicates the edges of low impedance thin beds,
- Hydrocarbon indicator by low frequency anomaly. This effect is some times accentuated by unconsolidated sands due to the oil content of the pores.
- Fracture zone indicator, they may appear as lower frequency zones.
- Chaotic reflection zone indicator, due to excessive scatter,
- Bed thickness indicator. Higher frequencies indicate sharp interfaces or thin shale bedding, lower frequencies indicate sand rich bedding.
- Sand/Shale ratio indicator in a clastic environment

Instantaneous frequency computed output is given in units of cycles per second. Instantaneous phase represents the phase of the resultant vector of individual simple harmonic motions. While individual vectors will rotate in clockwise motion, their resultant vector may, in some instances, form a cardioids pattern and appear to turn in the opposite direction. We interpret this as the effect of interference of two closely arriving wavelets. This can also be caused by the noise interference in the low amplitude zones. Because of these reversals, the instantaneous frequency will have unusual magnitudes and fluctuations.



Figure 4.12 Result Instantaneous Frequency in line 2905, Cantik field area, South Sumatra Basin

In some cases a frequency shadow may exist that indicate presence of gaseous phase in the reservoir that absorbing higher frequency content (Agustinus et al, 2005) (Figure 4.13). The sweetness attribute enhances the contrast between areas having subtly different net pay and porosity values when mapped using other attributes.

High values of net pay oil and porosity are shown to be associated with higher sweetness values (more than 2000). In return, an increasing “sweetness” value will be exhibited and can be qualitatively indicates carbonates-shale ratio.

But in this case, areas at surfaces of carbonate that filled by gas have indication a lower sweetness value (about less than 1000).

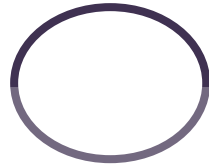


Figure 4.13 Result sweetness attribute in line 2905, Cantik field area, South Sumatra Basin

Since instantaneous frequencies are influenced by the bed thickness, we would like to observe them without too much interference. This we accomplish by using several adjacent traces to form a consistent output. It has been shown that instantaneous frequency, computed as the time derivative of instantaneous phase, relates to the centroid of the power spectrum of the seismic wavelet. From the time slice 1000 ms in Cantik field can define interesting areas (Figure 4.14). The black and red curve show that a paleo high area that have a high sweetness value. In that area well data was not appear because there was not infill well in there. Base on water cut bubble map, we can see the possibility that in that area is still intereting because oil was not producing from that area (Figure 4.15).

To see the relationship of Sweetness Attribute in fluid content, we can see the comparison between the amplitude map before sweetness attribute (Figure 4.16) and horizon slice of sweetness attribute in Baturaja Formation (Figure 4.17).

Figure 4.14 Result time slice sweetness attribute in time 1000 ms, show interesting area in Cantik field area, South Sumatra Basin

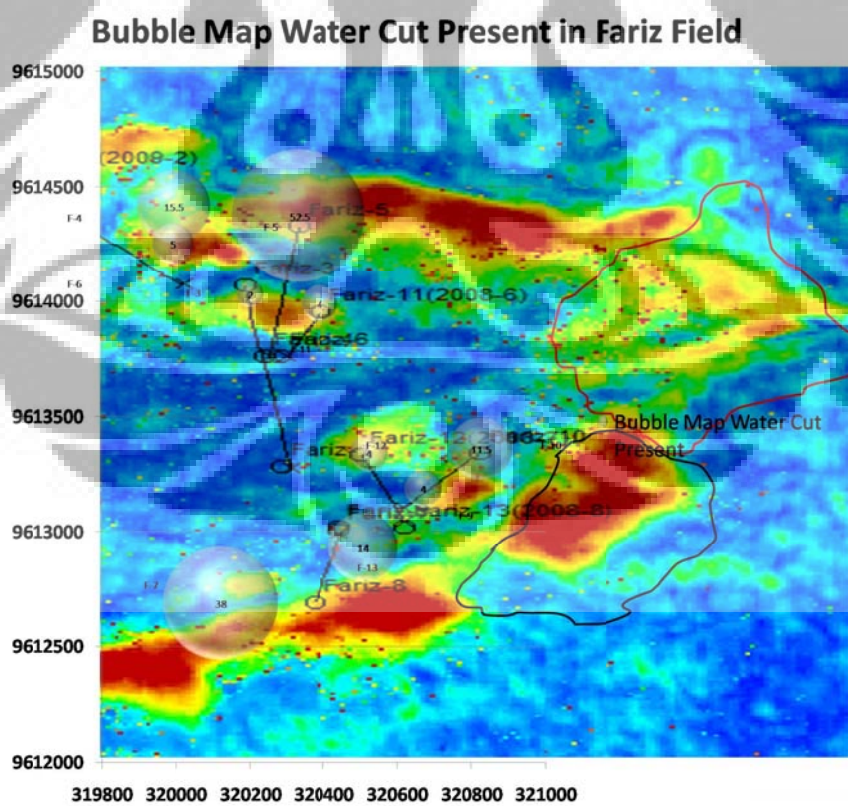


Figure 4.15 Overlay bubble map from water cut data and interesting area in Cantik field area, South Sumatra Basin



Figure 4.16 Result amplitude map in top of Baturaja Formation, show possibility of fluid content in Cantik field area, South Sumatra Basin

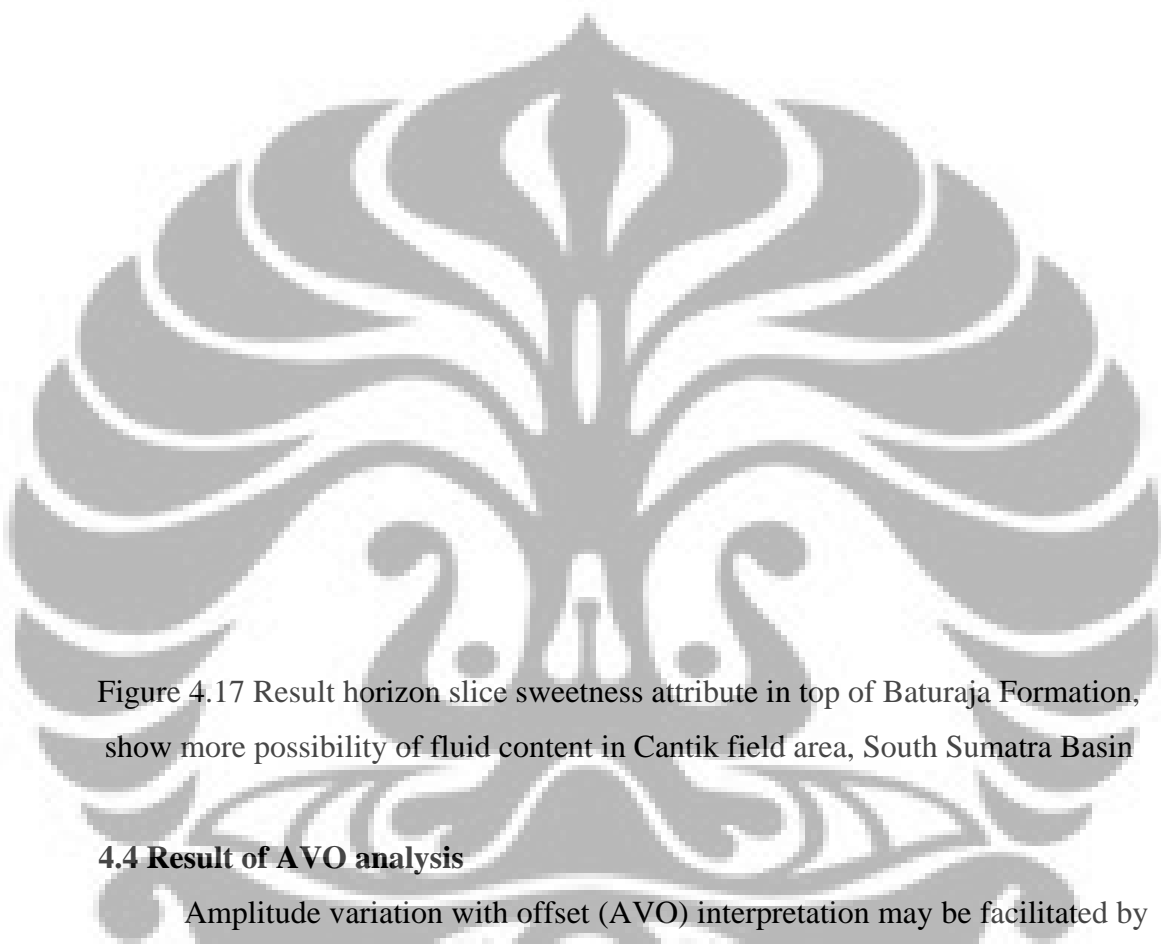


Figure 4.17 Result horizon slice sweetness attribute in top of Baturaja Formation, show more possibility of fluid content in Cantik field area, South Sumatra Basin

#### 4.4 Result of AVO analysis

Amplitude variation with offset (AVO) interpretation may be facilitated by crossplotting the AVO intercept ( $A$ ) and gradient ( $B$ ). Under a variety of reasonable petrophysical assumptions, brine-saturated carbonates and shales follow a well-defined “background” trend in the  $A$ – $B$  plane. Generally,  $A$  and  $B$  are negatively correlated for “background” rocks, but they may be positively correlated at very high  $V_P=V_S$  ratios, such as may occur in very soft shallow sediments. Thus, even fully brine-saturated shallow events with large reflection coefficients may exhibit large increases in AVO.

For doing the AVO analysis were define the gather data become steps. The first step define the super gather (Figure 4.18), after NMO corrections and angle gather (Figure 4.19) data was ready to used.

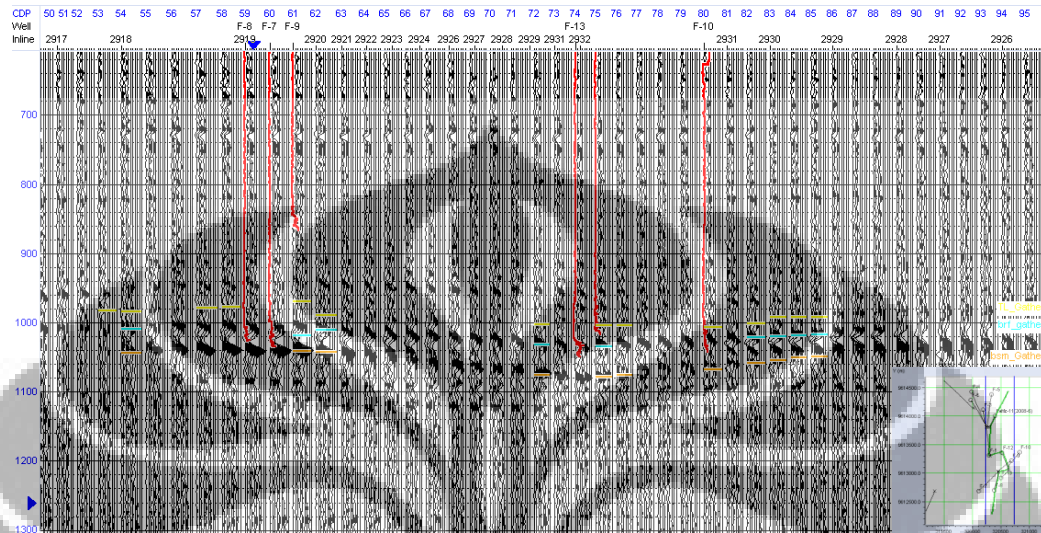


Figure 4.18 Super gather sections in arbitrary line trespassing wells in Cantik Field

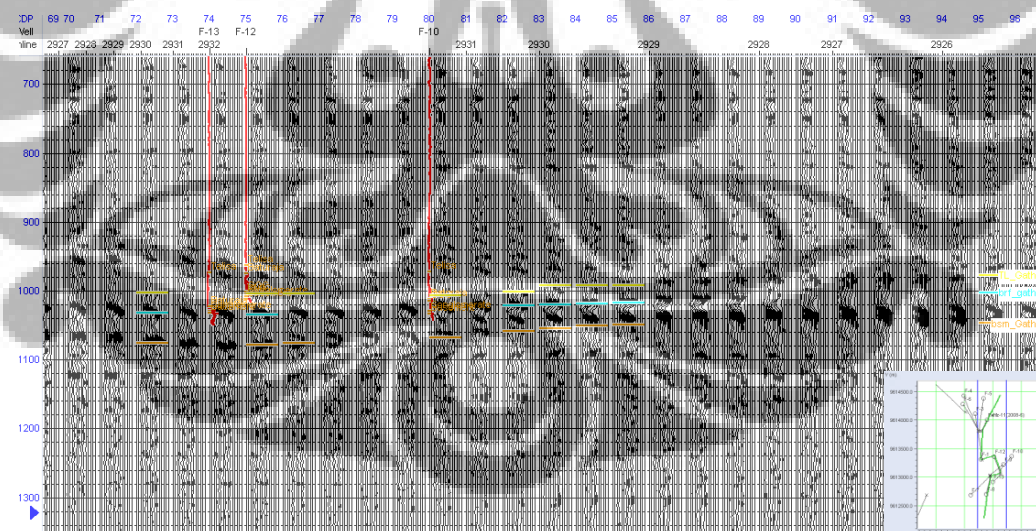


Figure 4.19 Angle gather section in arbitrary line trespassing wells in Cantik Field

The application of amplitude versus offset (AVO) in carbonate reservoirs is re-examined based on the increasing knowledge in the physical properties of carbonate rocks and advances in AVO technologies. The rock physics analysis indicated that porosity plays the dominating role in influencing carbonate rock

properties and suggests that gas effect may be determined using derived relations between velocities, porosity and gas effect. The amplitude vs. offset is calculated as a function of these effects in commonly encountered reservoirs (Figure 4.20). It is demonstrated that carbonate reservoirs have unique characteristics in amplitude variation with offset.

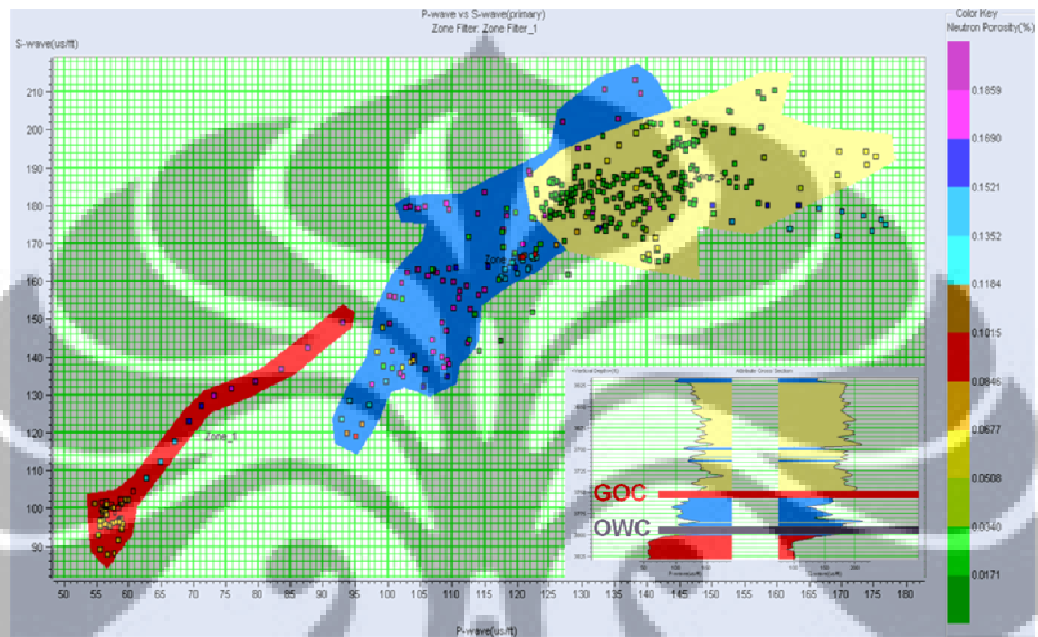


Figure 4.20 Crossplot result from well F-12, see the relationship result from fluid content, yellow was gas area; blue was oil area and red was water area

Deviations from the background trend may be indicative of hydrocarbons or lithologies with anomalous elastic properties. However, in contrast to the common assumptions that gas-carbonate amplitude increases with offset, or that the reflection coefficient becomes more negative with increasing offset, carbonates gas may exhibit a variety of AVO behaviors. A classification of gas sands based on location in the  $A-B$  plane (Figure 4.21), rather than on normal incidence reflection coefficient, is proposed. According to this classification, bright-spot gas sands fall in quadrant III and have negative AVO intercept and gradient. These carbonate exhibit the amplitude increase versus offset which has commonly been used as a gas indicator.



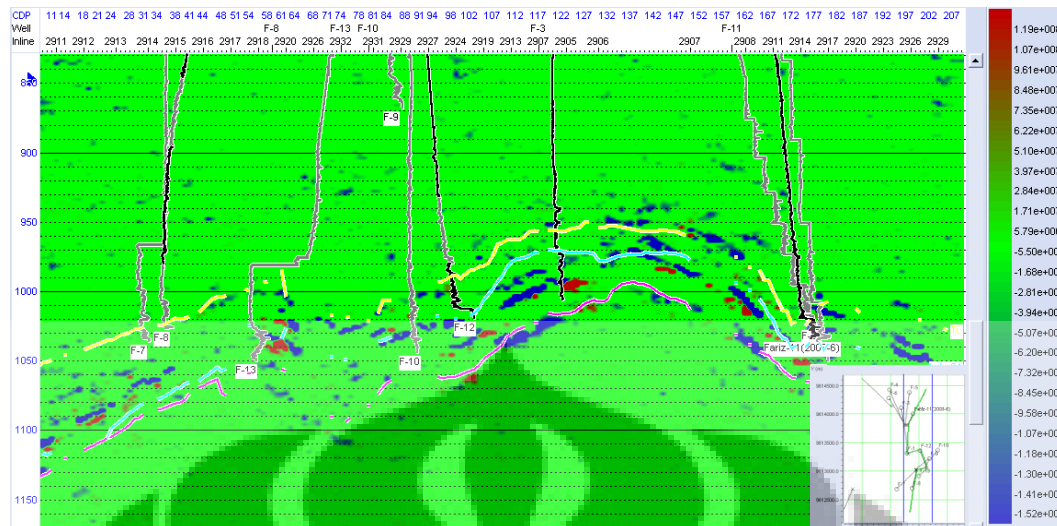


Figure 4.21 AVO result product  $A*B$  in arbitrary line trespassing wells in Cantik Field

High-impedance gas carbonates fall in quadrant II and have positive and negative AVO intercept AVO and gradient (Figure 4.22 and Figure 4.23). Consequently, these in carbonates case initially exhibit decreasing AVO and may reverse polarity. These behaviors have been previously reported and are addressed adequately by existing classification schemes. However, quadrant II gas carbonates have negative intercept and positive gradient. Certain “classical” bright spots fall in quadrant II and exhibit decreasing AVO. Examples show that this may occur when the gas-carbonates shear-wave velocity is lower than that of the overlying formation. Common AVO analysis methods such as partial stacks and product ( $A \times B$ ) indicators are complicated by this no uniform gas-carbonates behavior and require prior knowledge of the expected gas-carbonates AVO response. However, Smith and Gidlow’s (1987) fluid factor, and related indicators, will theoretically work for gas carbonate in any quadrant of the A–B plane.

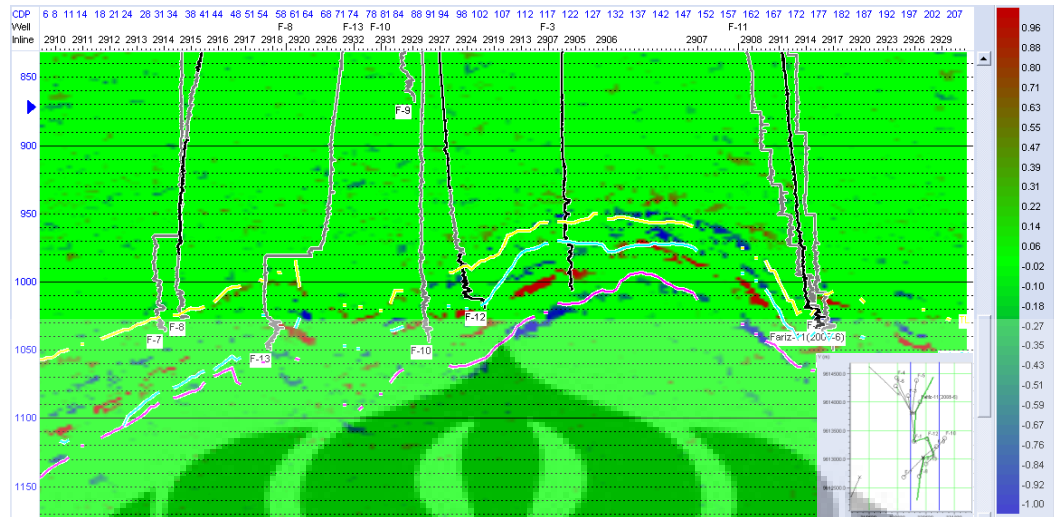


Figure 4.22 AVO result Intercept (A) in arbitrary line trespassing wells in Cantik Field

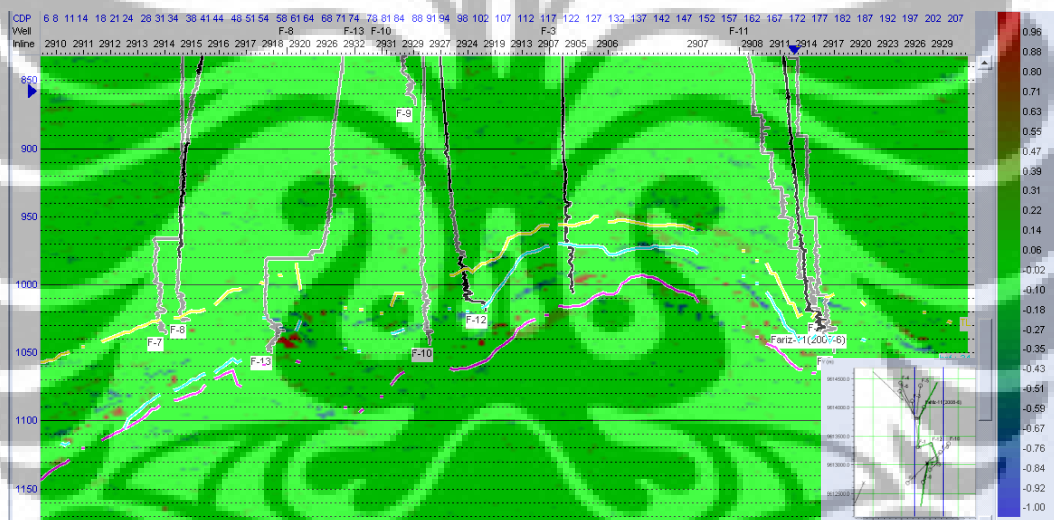


Figure 4.23 AVO result Intercept (B) in arbitrary line trespassing wells in Cantik Field

#### 4.5 Analysis of Validation between Sweetness Attribute and AVO Analysis

Validation result that we can see from sweetness attribute and AVO analysis result was area in east part of Cantik field very interesting. The sweetness attribute enhances the contrast between areas having subtly different net pay and porosity values when mapped using other attributes. High values of net pay and porosity are shown to be associated with higher sweetness values. In return, an increasing “sweetness” value will be exhibited and can be qualitatively indicates carbonates-

shale ratio. In some cases a frequency shadow may exist that indicate presence of gaseous phase in the reservoir that absorbing higher frequency content. From figure 4.24, we can define the frequency shadow at the flank area.

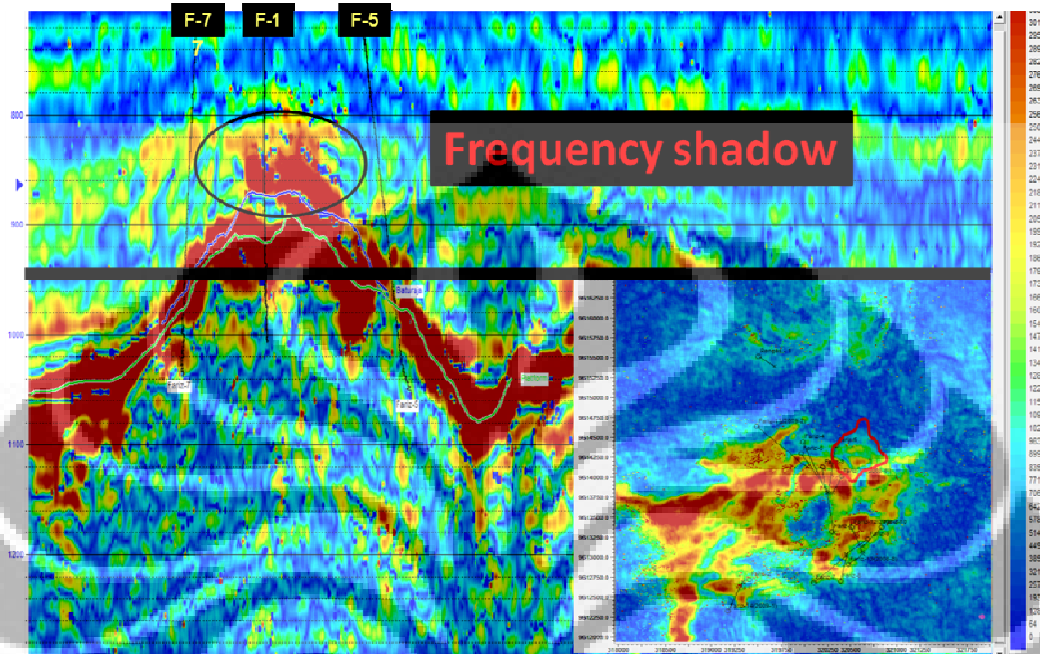


Figure 4.24 Sweetness result that show interesting area in the flank

After analyzed the sweetness attribute, we start to compare with AVO analysis. From fluid substitution result log data substituted by 100% gas top of Baturaja not changed, still in trough part, but when the log data substituted by 100% wet top of Baturaja changed become peak. From this result make higher confidence level that seismic interpretation base on well seismic tie before was already corrected. The P-wave depends only very weakly on the fluid saturation on account of the high mineral bulk modulus; this is not disturbed by a dynamic fluid substitution effect. Similarly, the fast shear wave behaves according to the Gassmann equation. The only real deviation from Gassmann occurs for the slow shear wave. This can be strongly influenced by the concept of dynamic fluid substitution. We are therefore led to the somewhat surprising conclusion that shear-wave splitting is potentially the attribute which is most sensitive to the saturating fluid in carbonate rocks.

Deviations from the background trend may be indicative of hydrocarbons or lithologies with anomalous elastic properties. However, in contrast to the common assumptions that gas-carbonate amplitude increases with offset, or that the reflection coefficient becomes more negative with increasing offset, carbonates gas may exhibit a variety of AVO behaviors. A classification of gas carbonates based on location in the  $A-B$  plane, in section of  $A*B$  product, intercept and gradient section we can see the distribution of interesting area. The interesting area has same location with the interesting area from sweetness attribute result. It made a big result that sweetness attributes powerful to become one approach to define fluid content.



## Chapter 5

### Conclusions and Recommendations

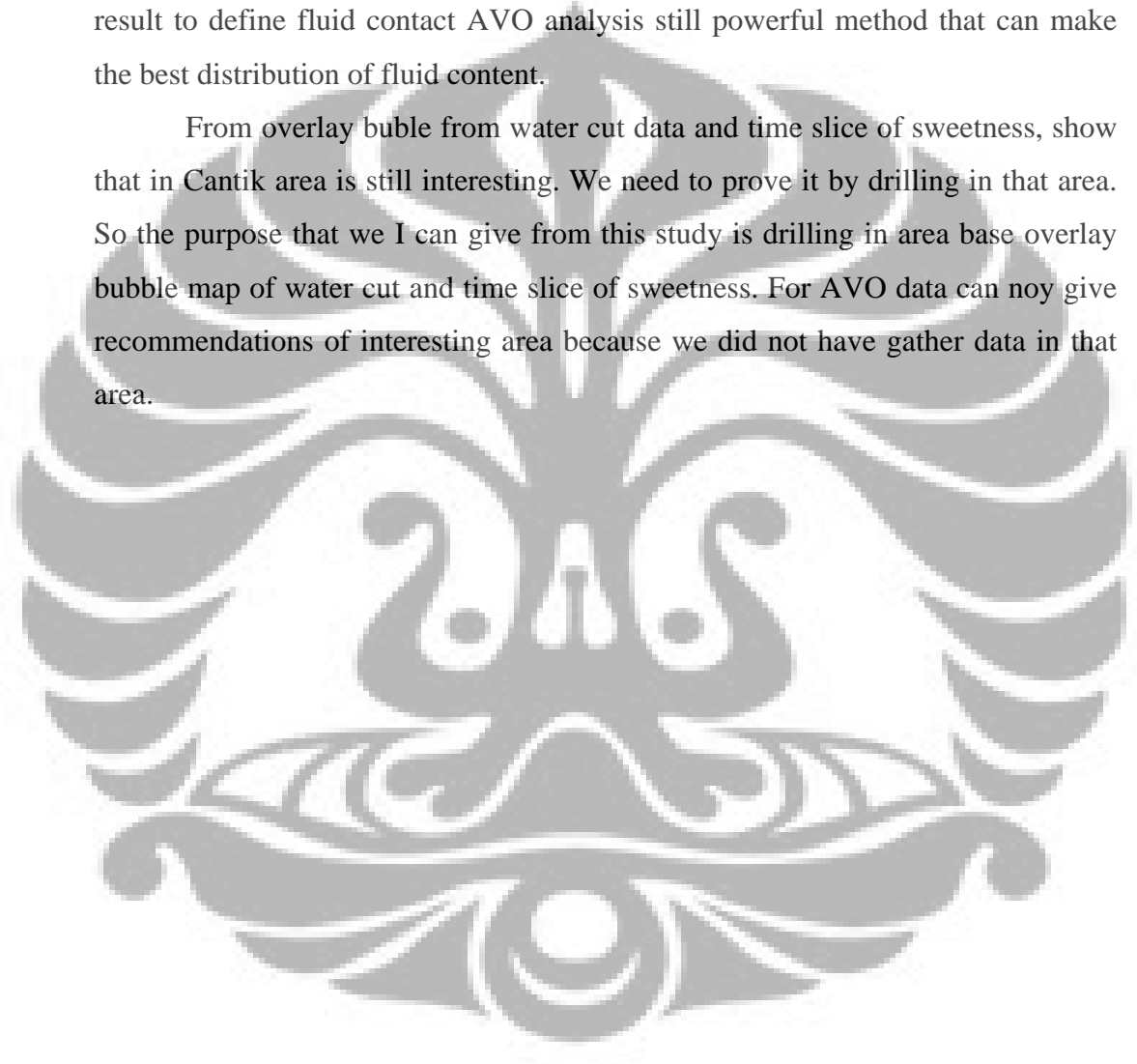
After analyzed the sweetness attribute, we start to compare with AVO analysis. From fluid substitution result log data substituted by 100% gas top of Baturaja not changed, still in trough part, but when the log data substituted by 100% wet top of Baturaja changed become peak. RC calculation in that area that also show same result. In well that have gas, RC price is negative and in well that have filled by oil is positive value. From this result make higher confidence level that seismic interpretation base on well seismic tie before was already corrected.

The P-wave depends only very weakly on the fluid saturation on account of the high mineral bulk modulus; this is not disturbed by a dynamic fluid substitution effect. Similarly, the fast shear wave behaves according to the Gassmann equation. The only real deviation from Gassmann occurs for the slow shear wave. This can be strongly influenced by the concept of dynamic fluid substitution. We are therefore led to the somewhat surprising conclusion that shear-wave splitting is potentially the attribute which is most sensitive to the saturating fluid in carbonate rocks.

Deviations from the background trend may be indicative of hydrocarbons or lithologies with anomalous elastic properties. However, in contrast to the common assumptions that gas-carbonate amplitude increases with offset, or that the reflection coefficient becomes more negative with increasing offset, carbonates gas may exhibit a variety of AVO behaviors. A classification of gas carbonates based on location in the  $A-B$  plane, in section of  $A*B$  product, intercept and gradient section we can see the distribution of interesting area. The interesting area has same location with the interesting area from sweetness attribute result. It made a big result that sweetness attributes powerful to become one approach to define fluid content.

We already know that preparation data to doing AVO analysis is very complex. We need a complete data, just like gather seismic data, well that have shear wave. And for the sweetness attributes we only need stack seismic data. If we want see from that point. We can see that sweetness attributes its can help us to define relative fluid content without need a complete data. Sweetness attribute can use by preliminary study to make fluid content distribution, but for the detail result to define fluid contact AVO analysis still powerful method that can make the best distribution of fluid content.

From overlay bubble from water cut data and time slice of sweetness, show that in Cantik area is still interesting. We need to prove it by drilling in that area. So the purpose that we I can give from this study is drilling in area base overlay bubble map of water cut and time slice of sweetness. For AVO data can noy give recommendations of interesting area because we did not have gather data in that area.



## REFERENCES

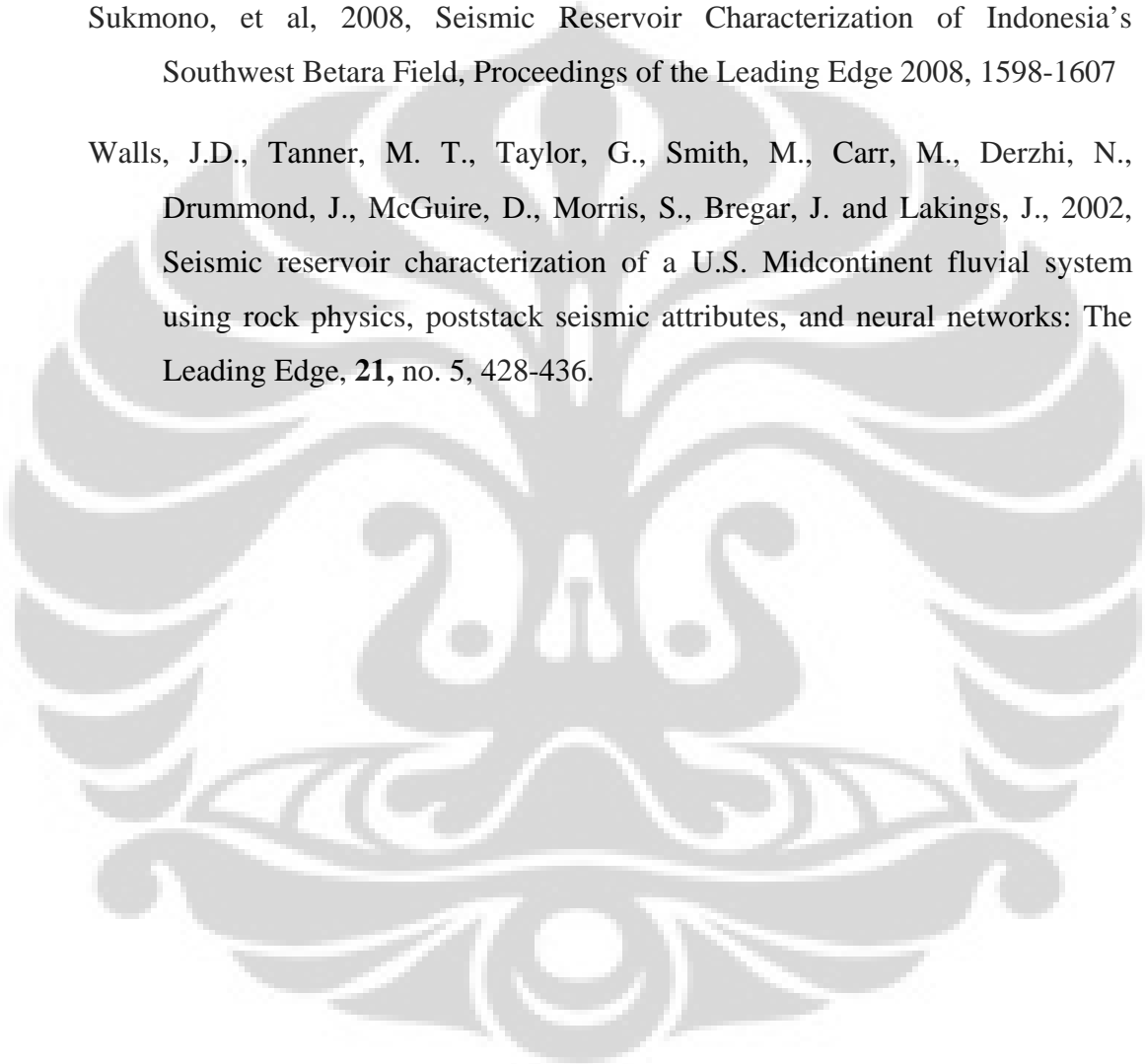
- Allen, J. L., Peddy, C. P. and Fasnacht, T. L., 1993, Some AVO failures and what (we think) we have learned: *THE LEADING EDGE*, 12, no. 03, 162-167.
- Brown, A. R., 1996, Interpreter's corner - Seismic attributes and their classification: *The Leading Edge*, **15**, no. 10, 1090.
- Castagna, J., 2000, An introduction to this special section: AVO--the next step: *The Leading Edge*, **19**, no. 11, 1187.
- Castagna, J. P. and Swan, H. W., 1997, Principles of AVO crossplotting: *The Leading Edge*, **16**, no. 04, 337-342. (\* Discussion in TLE-17-1-19 with reply).
- Coaster, De, G.L, 1974. Geology of the Central and South Sumatra Basins. IPA Proceedings, 3<sup>rd</sup> Annual Convention.
- Chopra, S., Alexeev, V. and Xu, Y., 2003, 3D AVO Crossplotting - An effective visualization technique.: *The Leading Edge*, **22**, no. 11, 1078-1089
- Hampson, D., 1991, AVO inversion, theory and practice: *The Leading Edge*, **10**, no. 06, 39-42.
- Hart, B. and Chen, M.A., 2004, Interpreter's Corner—Understanding seismic attributes through forward modeling: *The Leading Edge*, **23**, no. 09, 834-841.
- Kamal, Asril et.al, 2008. Field Trip Guide Book – GGT 2008, Internal report unpublished Medco E&P Indonesia.
- Nuryadin, Husni et.al, A Challenge and Future Potential of Basal Clastic Play in Paleo High, Musi Platform, South Sumatra Basin, IPA Proceedings, Jakarta 06-PG-23, 2006
- Russell, B. H., 1993, Introduction to AVO and this special issue: *The Leading Edge*, **12**, no. 03, 161.

Russell, B., Ross, C. P. and Lines, L., 2002, Neural networks and AVO: The Leading Edge, **21**, no. 3, 268-277.

SR. Agustinus, et al, 2005, Outstep Drilling Based on Geovolume Interpretation as Essentials Tool in Revitalizing a Brown Field, The Sangatta Oil Field, a Study Case, Proceedings of the IATMI National Symposium 2005, 2005-19

Sukmono, et al, 2008, Seismic Reservoir Characterization of Indonesia's Southwest Betara Field, Proceedings of the Leading Edge 2008, 1598-1607

Walls, J.D., Tanner, M. T., Taylor, G., Smith, M., Carr, M., Derzhi, N., Drummond, J., McGuire, D., Morris, S., Bregar, J. and Lakings, J., 2002, Seismic reservoir characterization of a U.S. Midcontinent fluvial system using rock physics, poststack seismic attributes, and neural networks: The Leading Edge, **21**, no. 5, 428-436.





## ATTACHEMENTS

TWT (ms)	Depth (meter)	Velocity
50	109.2	
343.1	155.18	12749
1000	366.42	6219.47
1100.1	398.98	6148.65
1200	431.22	6197.27
1299.9	462.66	6354.96
1400	496.01	6003
1500	528.42	6170.93
1600	560.49	6236.36
1700	591.58	6432.94
1710	594.55	6734.01
1820	628.37	6505.03
1900	652.59	6606.11
2000	680.12	7264.8
2100	711.67	6339.14
2200	738.68	7404.66
2300.1	768.62	6686.71
2400	797.7	6870.7
2500	828.94	6402.05
2600	857.97	6889.42
2699	885.66	7150.6
2800.1	913.08	7374.18
2900	938.76	7780.37
3000	942.37	55401.7
3100	992.67	3976.14
3200	1021.18	7015.08
3241	1030.85	8479.83
3354.1	1056.5	8818.71
3390.1	1076.42	3614.46
3400	1066.46	-1988
3416.1	1073.59	4516.13
3468.1	1088.93	6779.66
3485.1	1088.09	-40476
3524	1102.78	5296.12
3530.1	1107.16	2785.39
3587	1119.51	9214.57
3604.1	1125.51	5700
3650.2	1130.39	18893.4
3670	1133.14	14400

Table 1 Showing the checkshot data and calculating result of velocity based on checkshot data, the red column showed negative velocity

TWT (ms)	Depth (meter)	Velocity
50	109.2	
1000	366.42	7386.673
1100.1	398.98	6148.649
1200	431.22	6197.27
1299.9	462.66	6354.962
1400	496.01	6002.999
1500	528.42	6170.935
1600	560.49	6236.358
1700	591.58	6432.937
1710	594.55	6734.007
1820	628.37	6505.027
1900	652.59	6606.111
2000	680.12	7264.802
2100	711.67	6339.144
2200	738.68	7404.665
2300.1	768.62	6686.707
2400	797.7	6870.702
2500	828.94	6402.049
2600	857.97	6889.425
2699	885.66	7150.596
2800.1	913.08	7374.179
2900	938.76	7780.374
3200	1021.18	7279.786
3241	1030.85	8479.835
3354.1	1056.5	8818.713
3468.1	1088.93	7030.527
3524	1102.78	8072.202
3587	1119.51	7531.381
3650.2	1130.39	11617.65
3670	1133.14	14400

Table 2 Showing result after checkshot editing

Depth	GR	P-Wave	RHOB	Marker	RC
3360	67.73	98.566	2.423	TELISA	
3365	79.789	104.397	2.417		
3370	78.198	105.26	2.397		
3375	83.347	99.431	2.393		
3375.75	77.465	97.117	2.406		
3376	73.552	96.415	2.4	BATURAJA FORMATION	-0.00488
3380	54.075	96.864	2.171		
3385	54.366	110.135	1.82		
3390	44.023	107.867	1.907		
3395	42.999	105.37	1.833		
3400	46.719	105.087	2.041		
3405	36.324	109.927	1.932		
3410	35.035	105.522	1.891		
3415	32.518	100.422	2.107		
3420	34.552	109.747	1.871		
3425	47.854	112.519	1.897		
3430	27.997	106.369	2.007		
3435	31.542	104.958	1.934		
3440	49.351	104.116	1.932		
3445	24.899	76.583	2.461		
3450	20.967	76.225	2.304		
3455	26.246	80.574	2.062		
3460	41.656	98.976	1.955		
3465	40.634	105.532	1.941		
3470	31.057	95.982	2.049		
3475	29.298	98.426	2.029		
3480	32.296	101.732	2.064		
3485	24.751	96.117	2.01		
3490	21.378	89.091	2.241		
3495	22.093	79.558	2.345		
3500	22.171	90.561	2.06		
3505	22.226	101.305	2.019		
3510	42.975	94.42	2.011		
3515	27.09	102.011	2.176		
3520	31.736	104.554	2.003		
3525	24.395	93.008	2.208		
3530	28.318	105.471	1.969		
3535	47.126	87.58	2.141		
3540	34.484	97.133	2.024		
3545	67.679	87.612	2.399		
3550	26.961	102.524	1.938		
3555	20.16	101.831	2.017		

3560	35.882	104.107	2.112		
3565	21.566	100.053	2.002		
3570	22.681	101.121	2.112		
3575	25.64	85.841	2.156		
3580	29.742	93.344	2.16		
3585	28.163	90.049	2.262		
3590	34.041	73.228	2.34		
3592.75	108.745	67.678	2.39		
3593	112.472	68.227	2.387	BASEMENT	
3595	130.597	80.294	2.305		
3600	194.883	59.377	2.395		
3605	187.515	62.118	2.413		
3610	178.642	61.424	2.419		
3615	167.178	66.199	2.375		
3620	178.918	70.505	2.349		
3625	176.902	62.896	2.454		
3630	178.326	66.058	2.418		

Table 3 Showing result RC calculation in well F-1

Depth	GR	P-Wave	RHOB	Marker	RC
3371	106.3833	134.7334	2.211514	TELISA	
3372	107.406	131.4225	2.243318		
3373	105.908	132.2135	2.218523		
3374	104.7998	133.1119	2.185113		
3375	105.9381	135.0161	2.179976		
3375.5	108.7886	135.0163	2.189921		
3376	111.0773	134.6792	2.201926	BATURAJA FORMATION	0.001484
3380	114.9699	135.6825	2.226233		
3385	109.9165	134.1611	2.175361		
3390	112.939	153.8801	2.273374		
3395	119.0348	143.8649	2.266215		
3400	121.2491	137.3757	2.246468		
3405	127.1509	136.4414	2.274786		
3410	119.9293	140.1147	2.227524		
3415	114.4694	141.0366	2.213015		
3420	114.2643	140.4246	2.258789		
3425	112.6664	141.0743	2.285153		
3430	124.9534	140.1393	2.228863		
3435	118.2958	141.6887	2.195844		
3440	120.7395	140.4967	2.245678		
3445	121.6913	140.1293	2.232258		
3450	119.6601	138.7269	2.253093		
3455	119.8006	136.3139	2.239136		
3460	121.6133	139.7167	2.279147		
3465	126.2224	140.6062	2.242493		
3470	137.807	137.7294	2.224117		
3475	107.3702	138.4511	2.32171		
3480	108.9763	130.8907	2.226863		
3485	112.6538	139.1572	2.268645		
3490	115.0484	133.8196	2.242387		
3495	109.828	140.7016	2.261966		
3500	108.3791	136.6338	2.258655		
3505	103.3998	128.5058	2.288419		
3510	117.5295	145.0264	2.187653		
3515	117.681	136.837	2.220429		
3520	116.0562	135.3991	2.220819		
3525	115.319	135.9266	2.23186		
3530	119.6946	135.421	2.21326		
3535	113.4051	133.3363	2.229594		
3540	118.0211	135.9864	2.236159		
3545	116.0397	150.3191	2.25833		
3550	123.6438	136.7244	2.212715		

3555	113.2463	134.8173	2.231323	Blue	Purple
3560	109.0169	135.854	2.218024		
3565	117.395	137.9491	2.22605		
3570	105.5624	144.1703	2.189562		
3575	119.0523	137.6251	2.247855		
3580	119.6428	142.2398	2.265356		
3585	113.635	144.6479	2.256984		
3590	120.5133	141.4325	2.250582		
3592.5	118.8243	139.3143	2.261366		
3593	120.5953	138.715	2.245913		
3595	114.7937	139.641	2.243735		
3600	117.9282	139.0079	2.210168		

Table 4 Showing result RC calculation in well F-4

